JOURNAL OF MATERIALS SCIENCE 33 (1998) 3743–3762

Review
Shape-memory materials and hybrid composites for smart systems
Part I *Shape-memory materials*

Z. G. WEI, R. SANDSTRÖM
Department of Materials Science and Engineering, Royal Institute of Technology, S-100 44, Stockholm, Sweden
E-mail: ZGWEI@kth.se

S. MIYAZAKI
Institute of Materials Science, University of Tsukuba, Tsukuba, Ibaraki 305, Japan

A review is presented of the current research and development of shape-memory materials, including shape-memory alloys, shape-memory ceramics and shape-memory polymers. The shape-memory materials exhibit some novel performances, such as sensoring (thermal, stress or field), large-stroke actuation, high damping, adaptive responses, shape memory and superelasticity capability, which can be utilized in various engineering approaches to smart systems. Based on an extensive literature survey, the various shape-memory materials are outlined, with special attention to the recently developed or emerged materials. The basic phenomena in the materials, that is, the stimulus-induced phase transformations which result in the unique performance and govern the remarkable changes in properties of the materials, are systematically lineated. The remaining technical barriers, and the challenges to improve the present materials system and develop a new shape memory materials are discussed.

1. Introduction

During the past decade, smart materials and structures or intelligent material systems have received increasing attention because of their great scientific and technological significance [1–10]. Although the definitions of the terms *smart materials*, *smart structures*, *intelligent materials and structures* have not been reached to a consensus so far in the technical community [1, 11], it is now generally accepted that a *smart structure* is a structure system with macroscopically embedded or built-in sensors, actuators and is usually monitored or controlled by an external microprocessor or a computer. While, a *smart or intelligent material* refers to the material which has intrinsic sensing, actuating and controlling or information-processing capabilities in its microstructure. The smart materials and structures are supposed to be able to respond to environmental changes at the most optimum conditions and manifest their own functions according to the changes, that is, they can respond in a pre-determined manner and extent in an appropriate time with an environmental stimulus and then revert to their original states as soon as the stimulus is removed [1–3]. As is well known, few monolithic materials presently available possess these capabilities. Accordingly, intelligent or smart material systems are not singular materials, rather, they are hybrid composites or integrated systems of materials [1–5]. Amongst the advanced materials commercially available, some materials have multifunctions or primitive intelligence inherent in their structures, such as shape-memory alloys, piezoelectric ceramics, fibre-optics, magneto-(electro-)strictive materials, magneto-(electro)-rheological fluids and some functional polymers. To integrate and hybridize the advanced materials may lead to composite materials with intrinsic mechanisms for sensing, control and multiresponses.

Shape-memory materials (SMMs) are one of the major elements of intelligent/smart composites because of their unusual properties, such as the shape-memory effect (SME), pseudoelasticity or large recoverable stroke (strain), high damping capacity and adaptive properties which are due to the (reversible) phase transitions in the materials. SMMs may sense thermal, mechanical, magnetic or electric stimulus and exhibit actuation or some pre-determined response, making it possible to tune some technical parameters such as shape, position, strain, stiffness, natural frequency, damping, friction and other static and dynamical characteristics of material systems in response to the environmental changes. To date, a variety of

alloys, ceramics, polymers and gels have been found to exhibit SME behaviour. Both the fundamental and engineering aspects of SMMs have been investigated extensively and some of them are presently commercial materials. Particularly, some SMMs can be easily fabricated into thin films, fibres or wires, particles and even porous bulks, enabling them feasibly to be incorporated with other materials to form hybrid composites.

This review consists of two parts. Part I will outline various shape-memory materials and their basic characteristics, with special attention directed to the recent development trends and frontier areas. In Part II the design, fabrication, characterization and performance of various hybrid smart composites based on the shape-memory materials will be reviewed.

2. Shape-memory materials

2.1. Shape-memory alloys

2.1.1. Bulk shape-memory alloys

2.1.1.1. Ti–Ni system alloys. Although the discovery of shape-memory effect could date back to the early 1950s, the engineering significance of shape-memory alloys (SMAs) was not well recognised until the SME was discovered in the near-stoichiometric Ti–Ni alloys (Nitinol) in 1963 [12]. During the last three decades, the binary Ti–Ni alloys have been intensively investigated and nowadays are the most important commercial SMAs because of their exclusive shape-memory performance, good processibility, and excellent mechanical properties. In addition, the alloys have very good corrosion resistance and biocompatibility, which enable them to be widely used in the biomedical field. Because the Ti–Ni alloys can be readily fabricated into various forms or sizes, it is technically feasible to make them an active element in various composites. In particular, Ti–Ni thin films, fibres, particles and porous bulks have been successfully fabricated in recent years, and these materials, either in the monolithic form or in combination with other materials, have exhibited some exciting application potentials in microelectromechanical systems, medical implants, intelligent materials and structural systems. A more detailed introduction to the alloys can be found in the literature [13–23]. More recently, to meet some specific needs, which have arisen, some ternary alloys based on the Ti–Ni alloys have also been developed.

(a) *Narrow-hysteresis SMAs.* The substitution of copper for nickel in the near equiatomic Ti–Ni alloys has some interesting effects on their transformation behaviour, shape-memory characteristics and other properties: the one-stage transformation from cubic (B2) to monoclinic (B19′) in the binary alloy changes into a two-stage transformation from cubic (B2) to orthorhombic (B19) and from B19 to B19′ by substituting copper for nickel by more than 7.5 at %, meanwhile, the basic shape-memory capacity and the workability of the alloys are not appreciably deteriorated. By further substitution exceeding 10 at %, the alloys tend to proceed by one-stage transformation from B2 to B19, while the shape-recovery rate shows a slight decrease and the alloys become too brittle to be processed [24, 25]. Of particular interest are the following features: the ternary Ti–Ni–Cu alloys show less composition sensitivity of the martensitic transformation start temperature, M_s; the transformation hysteresis can be remarkably reduced from normally more than 30 K to less than 10 K; the dampening capacity ($\tan\delta$) can be increased to greater than 10^{-1}; and a larger difference in the toughness between the parent phase and martensite is produced. These features make the ternary $Ti_{50}Ni_{50-x}Cu_x$ (at %) alloys particularly suitable as actuator elements for smart systems [26–28].

(b) *Wide hysteresis SMAs.* Adding niobium to the binary Ti–Ni SMAs will depress the M_s temperature and can separate the start temperature for the reversion martensitic transformation A_s from M_s as far as 150 K. The wide hysteresis SMAs are quite desirable for coupling and fixing applications [29–32]; $Ti_{43}Ni_{47}Nb_9$ (at %) alloy is the most typical and commercially used one of the alloys. In the ternary alloys, only a small amount of niobium is dissolved into the B2 matrix, and most of it is presented in the form of niobium rich second phase which is supposed to be responsible for the widening of the transformation hysteresis [29–32].

(c) *High-Temperature SMAs.* When nickel in Ti–Ni SMAs is substituted by palladium, platinum and gold elements by up to 50 at % and titanium in Ti–Ni is substituted by hafnium and zirconium by up to 20 at %, the martensitic transformation temperatures can be increased to as high as 873 K while the basic shape-memory performance still exists [33–58]. These alloys are promising shape-memory alloys for applications at higher temperatures (> 393 K), despite their high cost. From an economical point of view, the Ni–Ti–Hf alloys are most attractive, and hence have been the most investigated in the last few years. The alloys have sufficient fabricability and their shape-memory capacity (recoverable elongation) is close to that of the binary Ti–Ni alloys. However, a systematic investigation of the phase stability of the alloys at elevated temperatures has not yet been undertaken. In some alloys, such as Ti–Ni–Au, it was reported that at high temperatures the ternary alloys are also susceptible to the ageing effects such as the martensite stabilization phenomenon [38].

2.1.1.2. Copper-based alloys. Copper-based shape-memory alloys have some advantages, such as low cost and simple fabrication procedure, compared to Ti–Ni alloys. Of the alloys, the ternary Cu–Zn–Al and Cu–Al–Ni alloys have been extensively studied and they are also now commercially available. The other commercial alloys include Cu–Al–Mn and Cu–Al–Be alloys. However, the applications of these alloys have been much limited mainly for two reasons: (1) the poor ductility and workability of the polycrystalline alloys resulting from the coarse grains, the high elastic anisotropy and the precipitation of brittle second-phase particles; and (2) the metastability of both the parent (B2, $D0_3$ or $L2_1$) and martensite (9R or 18R) phases in the alloys, which result in complicated ageing effects

and hence an undesirable reliability of the performance of the alloys [39–41]. Because Cu–Al–Ni alloys have a much better thermal stability and higher operating temperatures than Cu–Zn–Al alloys, they may become one candidate for practical high-temperature shape-memory alloys if only their poor processibility can be improved. In recent years, some efforts have been made to achieve this objective. As a result, some quaternary and pentatonic alloys based on Cu–Al–Ni, such as Cu–Al–Ni–Mn and Cu–Al–Mn–Ti(B) which has an M_s point greater than 423 K, have been developed [42–45]. Indeed, the workability of the Cu–Al–Ni alloys can be significantly improved by adding small amounts of alloying elements to the alloys, and cold-drawn wires can be produced [42–45]. However, the thermal stability of the alloys remains a crucial issue. Both martensite stabilization and parent-phase ageing effects were observed at temperatures greater than 393 K [42, 43].

2.1.1.3. Iron-base alloys. Because price is one of the key considerations for applications, the low-cost iron-based shape-memory alloys have attracted considerable attention in recent years, and now some of them are also close to a market introduction [46–48]. Of particular interest are Fe–Mn–Si, Fe–Cr–Ni–Mn–Si–Co, Fe–Ni–Mn and Fe–Ni–C. After complex thermomechanical treatments, these alloys exhibit perfect or nearly perfect SME due to the stress-induced martensitic transformation and the reversion, but usually only one-way SME of several per cent is achievable because the f c c austenite to the b c t or h c p martensite transformations in the alloys are not thermoelastic. In another interesting alloy, Fe–Ni–Co–Ti, the transformation from f c c austenite to b c t martensite is thermoelastic and a very high recovery stress (>1 GPa) can be achieved, with a fairly low thermal hysteresis (20–40 K) and transformation temperatures approaching ambient temperatures. More recently, the Fe–Pt and Fe–Pd alloys, which were previously investigated mainly as experimental materials, have received more attention again because the martensite transformations or the rearrangements of martensite variants in the alloys can be induced by magnetic fields and hence ferromagnetic shape-memory materials may be developed.

2.1.1.4. Intermetallic compounds. In the β-NiAl alloys with nickel contents of 62–69 at %, a thermoelastic martensitic transformation from B2 and $L1_0$ (3R) martensite occurs on quenching. The M_s temperature shows a strong dependence on the nickel content and on the solution-treatment temperature, and an M_s temperature of up to 503 K was recorded, indicating the potential use as high-temperature SMAs [34, 49–51]. To overcome the inherent brittle weakness, addition of third or fourth elements such as iron, manganese, boron, etc., to form a ductile second phase, and rapid solidification techniques such as melt-spinning, have proved to be effective, though at some expense of the SME [50]. Nevertheless, the Ni–Al alloys still suffer from phase metastability: Ni_5Al_3, Ni_2Al and an omega-like phase may precipitate at temperatures exceeding 523 K, worsening the shape-memory performance [34]. Some other β-phase intermetallic compounds, such as Ni–Mn and Ni–Mn–Ga [52]; Zr–Cu, Zr–Co, Zr–Rh, Zr–Ni and Zr–Co–Ni [53], Ti–V and Ti–V–Al [47, 54, 55], Gd–Cu, Tb–Cu and Y–Cu [56], also exhibit shape-memory effect and have some interesting potentials, but they are less technically mature and still under development.

During the past few decades, a great variety of shape-memory alloys have been extensively investigated. So far more than 5000 publications of SMAs have been recorded in the public literature, and the total number of applied patents using SMAs in different fields amounts to more than 4500 [13, 46]. Further information on the fundamental and engineering aspects of various SMAs can be found in many specific reviews [13, 19–23], books [14] and conference proceedings [15–18].

2.1.2. Thin-film shape-memory alloys

The bulk shape-memory alloys exhibit large strokes and forces but suffer from a slow response. This is due to the fact that SMAs are usually heat actuated, and this heat must be removed between cycles, and the cooling process usually results in a long cycle lifetime. Compared to bulk materials, SMA thin films provide a small amount of thermal mass to cool, and hence the cycle lifetime can be decreased substantially [57, 58]. As an excellent candidate for microelectromechanical systems (MEMS), SMA thin films have been of great concern in recent years because of their desirable mechanical properties, such as exerting a stress of hundreds of megapascals, tolerating strains of more than 3% working at common Transistor–Transistor Logic (TTL) voltages, and surviving millions of cycles without failure [59–63]. If SMA thin films are made on a substrate with good thermal conductivity such as silicon, the speed of operation may be increased to 100 Hz or higher [57, 61, 62]. More importantly, the composite multi-layers of these materials may be engineered into materials of micro-size dimensions, integrating materials science and electronic engineering into one functional chip which can be patterned with standard lithographic techniques and fabricated in batches [61–63]. Moreover, by coupling the SMA thin film with ferroelectric or ferromagnetic materials, SMAs may be actuated electrically or magnetically and smart composites with optimized characteristics can be obtained.

Andoh *et al.* [65] presented the first work on the deposition of shape-memory alloy films in 1986. They sputter-deposited Cu–Al–Ni films onto heated aluminium foils and the as-deposited films exhibited a good shape-memory effect. The fabrication of Ti–Ni SMA thin film was initially developed by Walker *et al.* [66], Busch and co-workers [67, 68], Ikuta and co-workers [69, 70] and Kuribayashi and co-workers [71, 72], with considerable contributions from several groups led by Grummon [73–76], Miyazaki [77–80], Jardine [57, 81–83] and Wuttig [84–86]. Up to now, Ti–Ni

[57–64, 66–101], Ti–Ni–Cu [61, 73, 75, 76, 102–107], Ti–Ni–Pd [103, 108], Ti–Ni–Hf [109, 110] and Cu–Al–Ni [65, 110] SMA thin films of up to 20 μm thickness have been successfully fabricated with direct current and radio-frequency magnetron sputtering [57–68, 77–110], plasma sputter deposition [76] and laser ablation processing [111] on to a variety of substrates. Most of the investigations have been performed on Ti–Ni and Ti–Ni–Cu alloys by magnetic sputtering and some reviews have been published [57, 61, 89]. The quality and the performance of the SMA thin films are mainly affected by metallurgical factors and deposition conditions [88, 91, 94]. Some crucial factors for the preparation and fabrication of SMA thin films are summarized below.

2.1.2.1. Control of composition. As is well known, binary Ti–Ni alloy is very sensitive to composition: a slight deviation (less than 1%) of nickel or titanium content from the stoichiometrically equi-atomic ratio of Ni : Ti can drastically alter the transformation temperatures [112, 113]. It is very difficult to control the alloy composition by using the conventional vacuum vapour deposition, though complete contamination-free conditions can be attained [111]. It was proposed that the laser ablation process can meet the needs of precise control of composition and minimized contamination [111], but the deposition rate is too slow (less than $0.02\,\mu m\,h^{-1}$) and the area of deposited thin film is limited. Contamination is a primary challenge when using the conventional sputtering process; however, precise compositional control is feasible by adopting proper manipulation, optimizing deposition parameters, pre-sputtering, coating the target with a layer of titanium or placing small titanium plates on the surface of target to lessen the target erosion, sputtering from multiple sources, either simultaneously or by alternating between different targets [61, 105]. On the other hand, it is feasible to deposit functionally gradient SMA films; Takabayashi *et al.* [114] have fabricated Ti–Ni films with a gradient composition and two types of crystal structure, namely, a nickel-rich layer and a titanium-rich layer, by r.f. magnetron sputtering with control of the input power to a titanium-target. Comparatively, ternary Ti–Ni–Cu alloys is of more interest because of their weak sensitivity to composition and a very narrow transformation hysteresis which make them more suitable as thin-film actuation materials.

2.1.2.2. Substrate temperature. The as-received films are amorphous if they are deposited on substrates at ambient temperature employing either sputtering or laser-ablation processing, and subsequently they must be annealed at temperatures greater than 723 K to crystallize, which invites complications related to interface diffusion and chemical reaction with components of the substrate [57, 61]. However, as-deposited crystalline films can be obtained if the substrate is heated during the deposition. For instance, Grummon *et al.* have successfully deposited crystalline Ti–Ni films with very fine grains by keeping the substrate temperature at around 703 K [87, 89]. The possible drawback of the hot-substrate deposition procedure may be that the produced films are liable to have porous or columnar microstructure, resulting in enhanced surface roughness [61]. Krulevitch *et al.* [61] have developed a procedure to produce high-quality SMA films on silicon substrates, while maintaining optimized shape-memory characteristics and low surface roughness: to deposit at a sufficiently high temperature (573 K) so that the film is in a dense amorphous or partially crystalline state, then anneal at a higher temperature (803 K) to promote grain growth and possibly recrystallization.

2.1.2.3. Sputtering gas pressure. The sputtering gas pressure has a critical effect on the characteristics of the films, though other process parameters such as sputter power, working distance and deposit incidence angle also affect them [68, 78, 88, 115, 116]. Generally ultra-high-purity argon gas is desirable and the typical working pressures range from 0.1–0.93 Pa (0.75–7 mTorr) [61]. Too low a working gas pressure cannot guarantee a successful deposition because of the extreme reactivity of the titanium, exploited technically in titanium sublimation pumps [57]. The films formed at too high pressures (6.7–13.3 Pa), however, suffer from porous structure and poor ductility [61, 88].

2.1.2.4. Contaminations. The environmental conditions inside the deposition chamber are also key factors affecting the quality of the films. A small amount of the impurities, including oxygen, hydrogen and carbon, will significantly deteriorate the shape-memory performance of the thin films [57, 61]. Therefore, the vapour pressures of oxygen, water and other reactive gases in the deposition chamber should be minimized. Another problem is the chemical interactions with the substrates during deposition and subsequent annealing. For instance, the silicon has a strong tendency to diffuse into Ti–Ni and form the nickel and titanium silicides when Ti–Ni films are deposited on silicon substrates and annealed at elevated temperatures [57, 58]. A proper buffer layer coated on the substrate and a minimal annealing temperature are effective for retardation of the interaction. This issue is of crucial concern when SMA hybrid multilayer composites are fabricated.

2.1.2.5. Thermal treatment. The as-deposited amorphous films on ambient temperature substrate must be annealed to crystallize to exhibit suitable shape-memory effect. The crystallization process must be monitored precisely in order to avoid or retard chemical interactions with the substrate, and the precipitation of second phases that deteriorate the SME of the film. The crystallization temperatures for Ti–Ni range from 723–973 K. Vacuum annealing at such temperatures for proper times generates excellent SME. Prolonged annealing or annealing at temperatures

above 823 K, however, readily leads to the formation of Ti_2Ni, Ti_3Ni_4 and $Ti_{11}Ni_{14}$ precipitates [57, 61, 95]. As a result, the shape-memory behaviour of the thin films is very sensitive to the annealing conditions. Taking into account that the SMA films may combine with dissimilar materials to form hybrid composites, the crystallization temperatures should be as low as possible. Jardine *et al.* [57] reported that the crystallization kinetics at 723 K were very slow, full crystallization occurring after a 7.5 h anneal. However, the crystallization temperature can be further lowered at 673 K through cold-working via rolling [57, 83].

2.1.2.6. Residual stress and adhesion. The residual stresses in the films will affect the mechanical behaviour and the static and dynamical compatibility with the substrates or dissimilar materials. Generally, the thin films deposited at low working gas pressure show large compressive intrinsic stresses. The biaxial residual stress, σ_f, in the film is given by the well-known Stoney equation [61]

$$\sigma_f = \frac{1}{6}\frac{E_s}{1-\nu_s}\frac{t_s^2}{t_f}\frac{1}{\rho} \quad (1)$$

Upon heating, the stresses increase in magnitude with increasing temperature and the rate of the stress evolution, $d\sigma/dT$ is determined by [116]

$$\frac{d\sigma}{dT} = \frac{E_f}{1-\nu}(\alpha_f - \alpha_s) \quad (2)$$

where E is the film modulus, α the coefficient of thermal expansion (CTE), ν the film Poisson's ratio, t the thickness, ρ the substrate radius of curvature, and the subscripts s and f refer to substrate and film, respectively. For the TiNi film deposited on (1 0 0) Si, the rate was estimated to be about $-1.5\,MPa\,K^{-1}$ [116]. The compressive stress tends to zero when approaching the crystallization temperature and then becomes a tensile stress of 50–100 MPa as a result of the film densification. The evolution of the high tensile stress may lead to cracking and delamination when annealing the amorphous SMA films on Si [89, 116]. However, the stress can be relaxed on cooling by the stress-induced martensitic transformation, and on heating a recovery stress will be generated, forming the basis for reversible cyclic actuation of the SMA/Si composites applicable to MEMS [57, 61, 89, 116, 117].

The deposited thin films can exhibit both perfect shape-memory effect and pseudoelasticity, and the thermomechanical properties are comparable to those of their bulk counterpart [61, 88, 91–94, 96]. A more specific review of the sputtering process, characterization of the microstructures and phase transformations, and the thermomechanical properties of the deposited SMA thin films will be presented in a separate paper [118].

2.2. Shape-memory ceramics

2.2.1. Visocelastic shape-memory ceramics

Some mica glass-ceramics exhibit clear shape-memory phenomenon, i.e., a nearly perfect recovery of up to 0.5% prestrain, after high-temperature plastic deformation, cooling under load to room temperature, and then reheating [119–124]. These materials typically have a heterostructure of a volume fraction of between 0.4 and 0.6 mica as the principal crystalline phase dispersed in a continuous glassy phase. Unlike shape-memory alloys, the shape-memory phenomenon in the heterostructure arises from the elastic energy introduced into the rigid matrix driving a viscous plastic strain reversal in the dispersed crystalline element on reheating. At temperatures above 573 K, the mica can be deformed plastically by basal slip and the plastic strain in the crystalline constituent accommodated elastically by the surrounding rigid glass. Because the glide through dislocations in mica is not possible at low temperature, the deformation of the material at elevated temperatures will be retained even if the load is removed, after cooling under load to ambient temperatures. The elastic strain energy stored in the glassy phase thus will provide a driving force for recovering the original shape. If the deformed mica is reheated to a high temperature at which the stored elastic strain energy is sufficient to activate the dislocation glide, the phase mixture will reverse the original plastic deformation. Fig. 1 shows the torsional strain recovery of a mica glass-ceramic as a function of time at several temperatures. The sample was deformed in axial compression at 773 K before cooling under load to room temperature, and a strain recovery of 99% was observed on prolonged annealing at 1073 K [120]. The viscoelastic shape-memory phenomenon is not limited to mica glass-ceramics or glass-ceramics. β-spodumene glass-ceramics and $2ZnO–B_2O_3$ glass-ceramics, and a variety of sintered ceramics that contain very little glass phase, including mica ($KMg_3AlSi_3O_{10}F_2$), silicone nitride (Si_3N_4), silicone carbide (SiC), zirconia (ZrO_2) and alumina (Al_2O_3), also exhibit the shape-memory behaviour [121–124]. However, the recoverable strain of the ceramics is much smaller (about 0.1%). Corresponding to the shape-recovery process, stress relaxation was observed. The activation energies for the shape-recovery process in the glass-ceramics were found to be much lower than those for high-temperature creep of the same mica glass-ceramics,

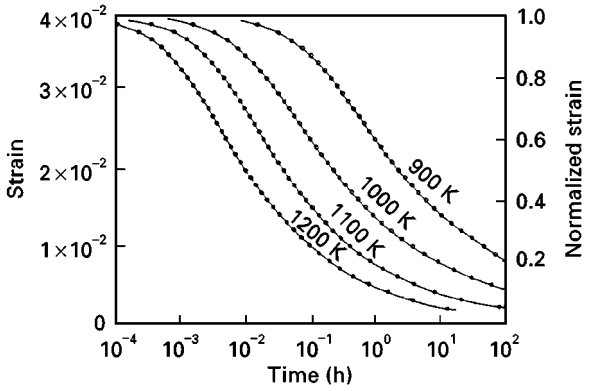

Figure 1 Torsional strain recovery of a mica glass-ceramic as a function of time. The material was deformed in axial compression at 773 K before cooling under load to room temperature, and then reheated to different temperatures [120].

thereby differentiating the two phenomena. Because the materials are visco-elastic and thermally stimulated, the shape-recovery percentage and shape-recovery force show a strong dependence on the prestrain, pre-deformation temperature, pre-deformation rate, reheating temperature and holding time [121, 123].

2.2.2. Martensitic shape-memory ceramics

Some inorganic or ceramic compounds undergo martensitic or displacive transformations which can be either stress or thermally activated, often resulting in transformation plasticity or transformation toughening. As a matter of fact, transformation toughening via the martensitic transformation is one of the most effective ways of improving the reliability and structural integrity of engineering ceramics, and has led to the wide recognition of the technological importance of the transformations in ceramics [125]. If the transformations in some ceramics are thermoelastic or ferroelastic, reversible strain or shape recovery, that is, pseudoelasticity and shape-memory effect can be expected. In certain ZrO_2-containing ceramics, the transformation between the tetragonal structure (t-ZrO_2) at intermediate temperatures and the monoclinic structure (m-ZrO_2) at low temperatures, can occur thermoelastically [125]. The magnesia-partially stabilized zirconia (Mg-PSZ) [119, 126] and the ceria-stabilized, tetragonal zirconia polycrystals (CeO_2–TZP) [119, 127–129] have been reported to show shape-memory behaviour. In the CeO_2–TZP, the t–m transformation occurs at a characteristic temperature M_b on cooling, which depends on the grain size. The t–m transformation can also be stress-induced at temperatures above M_b, resulting in seemingly "plastic" deformation. On subsequent reheating, the m–t transformation occurs and the strain can be recovered. Fig. 2 shows the shape-memory effect observed in a ZrO_2–12 mol % CeO_2 ceramic. In the ceramic, total strains up to 1.5%–2% in uniaxial compression can be almost fully recovered, but significant grain-boundary microcracking and other irreversible damage occur which lead to a degradation in shape recovery and premature fracture. However, a near full shape recovery of axial compressive plastic strains of up to 4.5% can be achieved while the tendency of microcracking be suppressed in the samples deformed in hydraulic compression [119, 127]. More displacive or martensitic-like transformations and potential shape-memory materials can be found in a variety of structural ceramics [130, 131]. In addition, some ionic materials such as $Pb_3(PO_4)_2$ and $LnNbO_4$ (Ln = La, Nd), crystals [132–136], and some superconductors such as V–Si and Zr–Hf–V [137], Y–Ba–Cu–O, Bi–(Pb)–Sr–Ca–Cu–O and Ti–Ba–Ca–Cu–O [138–141], also exhibit remarkable pseudoelasticity and shape-memory effect, due to first-order martensitic transformations or the rearrangements of the ferroelastic domains in the materials. Using the ceramics, some new shape-memory device can be designed for high temperature application where ordinary shape-memory alloys are not applicable. However, the technological application of the shape-memory capacity is limited by the small magnitudes of recoverable strains and the tendency of the ceramics to microcracking.

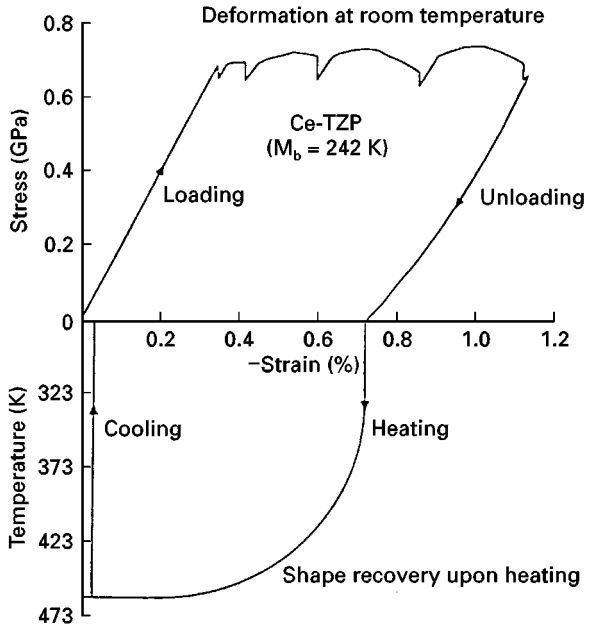

Figure 2 Axial stress–strain curve for ZrO_2-12mol.%CeO2 under uniaxial compression at room temperature, together with temperature–strain curve showing strain recovery on subsequent heating [129].

2.2.3. Ferroelectric shape-memory ceramics

In pervoskite-type oxides, the crystallite domains may exist in a variety of states such as cubic, tetragonal, rhombohedral or orthorhombic, which may be either paraelectric, ferroelectric or antiferroelectric, depending upon the exact composition, as well as external conditions such as temperature, stress and electric field. The phase transitions between the different structures, such as the paraelectric–ferroelectric (PE–FE) transition and the antiferroelectric–ferroelectric (AFE–FE) transition, may be accompanied by a considerable strain in the ceramics. In particular, it has been observed that the orthorhombic antiferroelectric (AFE) to tetragonal ferroelectric (FE) transition in some ceramics usually generate large strains [119, 142–148]. Very importantly, in suitable compositions, the AFE–FE transition can be induced by application of a sufficiently large electric field. The phase transition, which is caused by the switching or reorientation of the polarized domains, is accompanied by a lattice distortion leading to a linear "digital" displacement and a net volume expansion [146, 147]. Because the total strain is comprised of (i) a spontaneous strain which occurs due to the phase transformation, and (ii) a strain associated with domain alignment on poling, the induced strain is much larger than that resulting from the converse piezoelectric effect in the conventional piezoelectrics. Total strains of up to 0.6% have been reported to occur during the transition [144, 146]. When the electric field is removed, conventional electroceramics will return to their original state. This is a typical

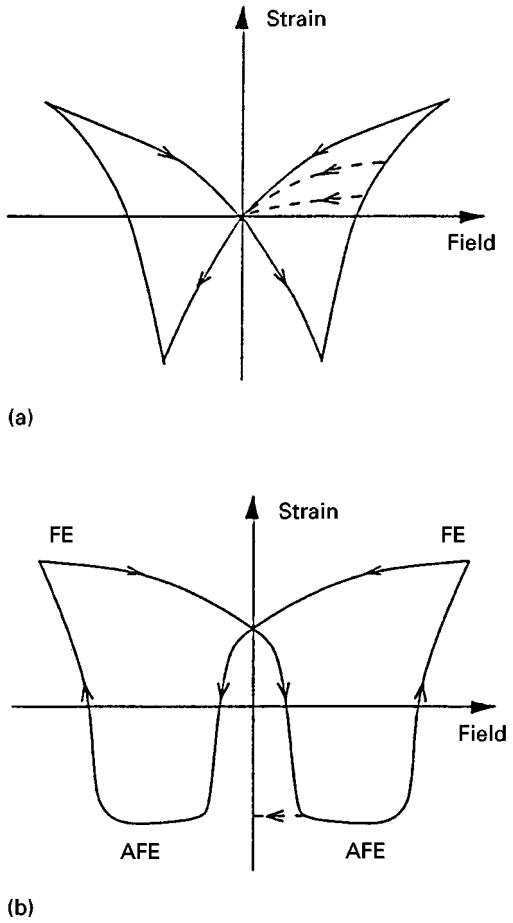

Figure 3 Comparison of the longitudinal strains for ferroelectric and antiferroelectric materials. (a) Spontaneous strain due to polarization in a ferroelectric, (b) field-induced transformation strain from AFE to FE state [148].

ferroelectric behaviour. Some ceramics, however, are metastable in either of the ferroelectric and antiferroelectric states at zero field, and they will remain in the ferroelectric state as the field is removed. To return to their original states, it can be achieved either rapidly by reversing the polarity of the applied field, or slowly by heating to effect the reverse FE–AFE transformation, thus giving rise to a shape-memory behaviour similar to those observed in shape-memory alloys. Fig. 3 shows a comparison of the filed-induced strains for ferroelectric and antiferroelectric materials. The shape-memory effect has been observed in the perovskite-type oxides (Pb, La) (Zr, Ti)O_3 (PZSTs) [119, 142, 143], Pb(Zr, Sn, Sn, Ti)O_3 (PZSTs) [119, 142, 144, 145], (Pb, La) (Zr, Sn, Ti)O_3 (PLSnZTs) and (Pb,Nb) (Zr, Sn, Ti) O_3 [146–150], (Sr, Ba) Nb_2O_6 [151] and the hexagonal manganites $RMnO_3$ (R = Ho, Y) [152]. Although the shape-memory ceramics have lower strain levels than shape-memory alloys, they have some clear advantages and may be more suitable for certain applications. For instance, because an electric field can be readily changed at much higher rates than temperature, the shape-memory ceramics may be actuated at higher bandwidths, with the maximum response speed of only a microsecond [142]. A prototype adaptive structure using the shape-memory ceramics has been demonstrated by Ghandi and Hagood [147, 148].

2.2.4. Ferromagnetic shape-memory ceramics

Some transition metal oxides undergo paramagnetic–ferromagnetic, paramagnetic–antiferromagnetic transformation, or orbital order–disorder transitions and the reversible transformations are also accompanied by recoverable lattice distortions. In the tetragonal manganite spinels $Mn_x(Zn, Cd)_{1-x}Mn_2O_4$ [153, 154] and in the non-stoichiometric orthomanganites $RMnO_{3+x}$(R = Nd, Sm, Eu, Gd, Tb, Dy) [155], the orbital ordered and disordered phases coexist in a wide temperature interval, and short-range ferromagnetic (or antiferromagnetic) ordering or Jahn–Teller phase transitions may take place, resulting in a shape-memory effect. Because, most of the manganites are antiferromagnets and their Néel temperatures are very low, spontaneous magnetization of the compounds is only achievable at very low temperatures. As a result, the effects of magnetic field on the transformation and ferromagnetic shape-memory effect in the compounds are less investigated.

2.3. Shape-memory polymers and gels

Shape-memory polymers (SMPs) were introduced in 1984 in Japan, and have since gained much attention in Japan and in the United States [156, 157]. It is well known that polymers exist in a rubbery state at higher temperatures and in a glassy state at lower temperatures. Owing to the lower rubbery modulus, polymers can be subjected to a very large deformation at higher temperatures. Because the glassy modulus is at least two orders of magnitude times the rubbery modulus, the stored elastic stress is not large enough to drive the reverse deformation in the glassy state as the load is removed. As a result, the deformation can be frozen in the glassy state on quenching or after cooling under load to the lower temperatures. Usually, ordinary polymers cannot completely restore their residual inelastic deformation upon reheating to the rubbery state. In contrast, shape-memory polymers can recover almost all the residual deformation. These polymers typically consist of two phases, namely fixed phase and reversible phase. Amongst them, the polynorborene, the trans-isopolyprene and the styrene–butadiene copolymer were the first few polymers reported to exhibit shape-memory effect. However, the commercial application of the early-developed shape-memory polymers were much limited because of their undesirable properties, namely a narrow range of glass transition temperature, T_g, and poor processibility [157–159].

More recently, segmented polyurethane thermoplastic polymers have received intensive attention [156–160]. They are usually polymerized from diphenylmethane diisocyanate (OCN–R–NCO) and polycaprolactone diols (HO–R′–OH), with butanediol (HO–R″–OH) as chain extenders. The polyurethane are thus basically multiblock copolymers consisting of alternating sequences of soft segments with molecular

weight 1000–10000, and hard segments which are built from diisocyanates and extenders, as follows [161]

$$\underset{\text{(soft segment, polyol)}}{H\text{–}[O\text{–}(CH_2)_5\text{–}CO\text{–}]_n\text{–}O\text{–}R}\text{——}\underset{\text{(hard segment, diisocyanate + extender)}}{OOCHN\text{–}R'\text{–}NHCOO\text{–}R''\text{–}OOCHN\text{–}R'} \quad (3)$$

In the polyurethane, the hard segments aggregrate and form the physical cross-linking points through polar interaction, hydrogen bonding, and crystallization. Such cross-linking points cannot be broken at temperatures below 393 K [162]. Meanwhile, the soft segment domains form the reversible phase and the observed shape-memory effect is due to the molecular motion of the soft segments. Depending on the molecular weight of the soft segment, the molar ratio of the soft segment to hard segment and the manufacturing procedure of the resins, the static and dynamic properties of the polymers are easily controlled, and the shape-recovery temperature can be freely tailored in the range of room temperature ± 50 K to meet the requirements of a specific application. Moreover, the segmented polyurethanes have improved processability, can be processed using conventional techniques including injection, extrusion, blow moulding and solution coating to contain complicated shapes. Because the cross-link in the polyurethane is not chemical, the SMPs have excellent chemical properties. They do not dissolve in any acid or base. In soaking tests in water, gasline and detergent solution, they demonstrated fairly good chemical resistance. After long time (300 h) sunshine exposure, negligible change in properties such as modulus was observed [158]. Also, the materials exhibit excellent medical bio-compatibility [159].

The typical value of the elastic modulus of the SMPs is about 827 MPa (120×10^{-3} p.s.i.) in their glassy state and 2 MPa (300 p.s.i) in their rubbery state [158]. In some SMPs, the modulus ratio of the glassy state to the rubbery state may exceed 500. As regards shape-memory capacity, strains of more than 400% can be recovered in the materials. SMPs also demonstrate visco-elastic behaviour: their internal loss factor can be as high as 0.5–1.0 at their glass transition temperatures, and their stress-strain curves are greatly affected by strain rate [158]. The structure–property relationships and the thermomechanical behaviour of the polyurethane have been systematically examined by several researchers [158–166]. The negative aspect of the SMPs may be their low recovery force. When small amounts of stress (< 4 MPa) are applied to the polyurethane components, the shape-recovery property is lost. Therefore, the SMPs are usually used in the cases where only free recovery or very low recovery force and mechanical strength are addressed. Nevertheless, SMPs have several distinct advantages such as low density ($1.0–1.3 \times 10^3$ kg m^{-3}), high shape recoverability (maximum strain recovery > 400 %), easy processability, transparent (hence can be coloured), and economical, compared with SMAs. With on-going elaborations on improvement in their mechanical properties, the shape-memory polymers are expected to find more applications.

During the last decade, many contractile polymeric gels, namely intelligent gels, have been developed [167–170]. These gels consist of an elastic cross-linked network and a fluid filing the interstitial space of the network, and therefore can easily change their size and shape and in turn result in a shrink or swell in response to infinitesimal changes in environmental conditions such as temperature, light, ion, pH, solvent concentration, biochemical element, small electric field and stress, depending upon the precise structure of the gel and the chemical composition of the solvent and gel [168, 169]. They are a unique chemomechanical system that is capable of conversion between chemical energy and mechanical work. By undergoing phase transitions which are accompanied by reversible, continuous or discrete volume changes by three orders of magnitude, the gels can provide actuating power capacities comparable to that of human muscles [171, 172]. Moreover, the soft materials exhibit such a pliant movement that is usually observed only in the natural biological systems [167]. Through spatial modulation of the chemical nature of gels, smart gels with shape memory effect, and composite gels which are responsive to multi-stimuli can be synthesized [172, 173]. The main shortcomings of the gels are their undesirable chemical hysteresis and mechanical hysteresis.

3. Basic phenomena: phase transformations

3.1. Thermally induced transformations

The shape-memory alloys and ceramics undergo diffusionless martensitic transformations on cooling beyond critical temperatures, M_s, which are dependent upon alloy composition, processing procedures and thermal/mechanical treatment conditions. The phase transformations between the high-temperature parent phase and the low-temperature martensite in most of the SMAs (excluding some iron-based alloys) are thermoelastic [13, 18]. In the binary Ti–Ni and some TiNi-base ternary alloys, a second order-like R-phase transition occurs, while in most of the other β-phase SMAs, the nearest-neighbour (B2) and second nearest-neighbour ($D0_3$, $L2_1$) atomic ordering transitions will take place, prior to the formation of the long period stacking order martensite structures. These transitions either have their own potentials to be utilized separately or have an important effect on the subsequent martensitic transformations [26, 40, 174]. In SMPs, a glass transition occurs between the high temperature rubber state and the low-temperature solid state across a narrow transformation bandwidth (10–30 K). Almost all the phase transitions in polymeric gels show a strong temperature dependence, and the so-called light-induced phase transitions in some gels are, in fact, thermally induced transitions [168, 169]. The ferroelectric and the ferromagnetic

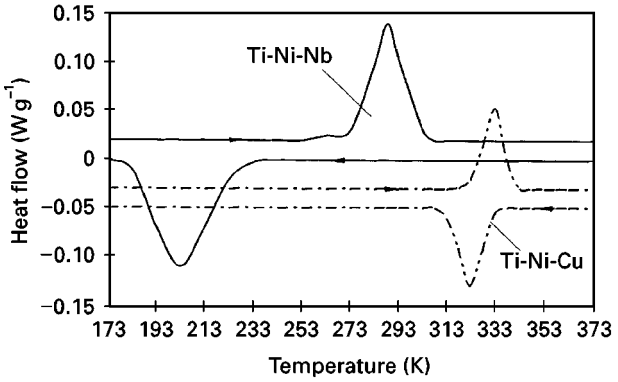

Figure 4 DSC curves showing the transformations in the (—) wide hysteresis $Ti_{43}Ni_{47}Nb_9$ and (–·–) narrow hysteresis $Ti_{50}Ni_{25}Cu_{25}$ shape-memory alloy.

shape-memory ceramics will undergo the paraelectric–ferroelectric (or antiferroelectric) transformation and the paramagnetic–ferromagnetic (or antiferromagnetic) transformation on cooling through the Curie (or the Néel) temperature, respectively. Both states of long-range and short-range chemical or magnetic atomic order in the materials may play an important part in the behaviour of the materials.

Because the martensitic transformations in the materials are of the first-order type, the forward transformation and the reversion exhibit an exothermic heat and an endothermic heat (transformation enthalpy), respectively. As a result, a thermal hysteresis, which depends on the material composition and microstructure, exists between the forward and the reverse transtition, ranging from several Kelvin to more than 100 Kelvin. Besides the transformation temperatures, the transformation enthalpy and the hysteresis are two important factors of concern in materials design and engineering applications. For instance, the SMAs with narrow hysteresis, such as Ti–Ni–Cu and Mn–Cu alloys, are desirable for rapid and precise actuation control, whereas the alloys with large transformation enthalpy and wide hysteresis, such as Ti–Ni–Nb and some iron-base alloys, are suitable for coupling or fastening applications. Fig. 4 shows the differential scanning calorimetry (DSC) curves demonstrating the forward and reverse martensitic transformations in the narrow hysteresis Ti–Ni–Cu and wide hysteresis Ti–Ni–Nb alloys. The temperature-induced phase transitions which can be tailored via composition design and processing procedures enable the materials to have the native capabilities of thermal sensing, and switch-on or switch-off control.

At present, the most widely used smart materials are piezoelectric ceramics, electrostrictive ceramics, magnetostrictive materials and ferroelastic shape–memory alloys. Very interestingly, as noted by Newnham [175], these materials have many features in common: all of them have a cubic lattice at high temperatures and undergo either a chemical or a ferromagnetic/orbital ordering transition; when cooling to ambient temperatures they all are poised near a morphotropic phase boundary which is characterized by a displacive transition accompained by significant atomic displacements and electromechanical coupling; more importantly, they are all ferroic with active domain walls which can be triggered by stress and fields. Fig. 5 shows the phase diagrams of three prototypes of smart materials: (a), piezoelectric $Pb(Zr,Ti)O_3$, (b) magnetostrictive (Tb,Dy) Fe_2 (Terfenol-D), and (c) ferroelastic Cu–Zn–Al SMA. $Pb(Zr,Ti)O_3$ has the ideal cubic perovskite structure at high temperature. On cooling below the Curie point, it converts from the paraelectric state into a ferroelectric tetragonal phase. Of more importance is the second transition from the tetragonal to rhombohedral phase. Although both the phases are ferroelectric, they have different poling directions. Very large piezoelectric coupling between electric and mechanical variables is obtained near this phase boundary [175]. Terfenol-D is cubic and paramagnetic at temperatures above 700 K; below the Curie temperature it transforms into a rhombohedral structure with magnetic spins aligned along $\langle 111 \rangle$ direction. Like PZT, it is poised on a rhombohedral–tetragonal phase boundary at room temperature, with the spins ready to switch into the tetragonal direction [176]. The Cu–Zn–Al alloy is also cubic at high temperatures, with a B2 ordered structure derived from disordered b c c. Like many Heusler alloys it undergoes the second nearest-neighbour atomic ordering transition at T_c'. Near room temperature, it is poised on the phase boundary between the ordered parent phase and the rhombohedral (or monoclinic) martensite with an internally twinned substructure. Generally, the martensitic transformations in most SMAs are athermal transformations, but in some alloy systems, under certain conditions such as applying a stress or pressure, the athermal transformations can change into isothermal transformations [177, 178]. From a thermodynamic point of view, the unstable state of the materials poised near to the phase boundary makes it possible to trigger or switch a transformation by stress, field as well as thermal stimuli for the low-energy barrier. As a result, this metastability ensures persistent disequilibrium over a wide range and optimizes dynamic behaviour by staying on the edge of rapid response [175]. To seek more desirable morphotropic transitions and set the compositions near the phase boundaries will be one of the guidelines in the design of more smart materials. The recent development of electric field-induced shape-memory ceramics has clearly demonstrated this point. Also, it should be mentioned that at low temperature, all the afore-mentioned materials have a crystal structure with a lower symmetry than the cubic, such as rhombohedral, monoclinic and tetragonal. This crystallographic feature can favour the domains associated with dipoles and strains to orient or reorient along certain directions, thus giving rise to a large displacement. These remarkable similarities between the typical materials shed some light on the future development of new smart materials.

3.2. Stress- and pressure-induced transformations

The martensitic transformations in shape-memory alloys and ceramics can be stress induced if only

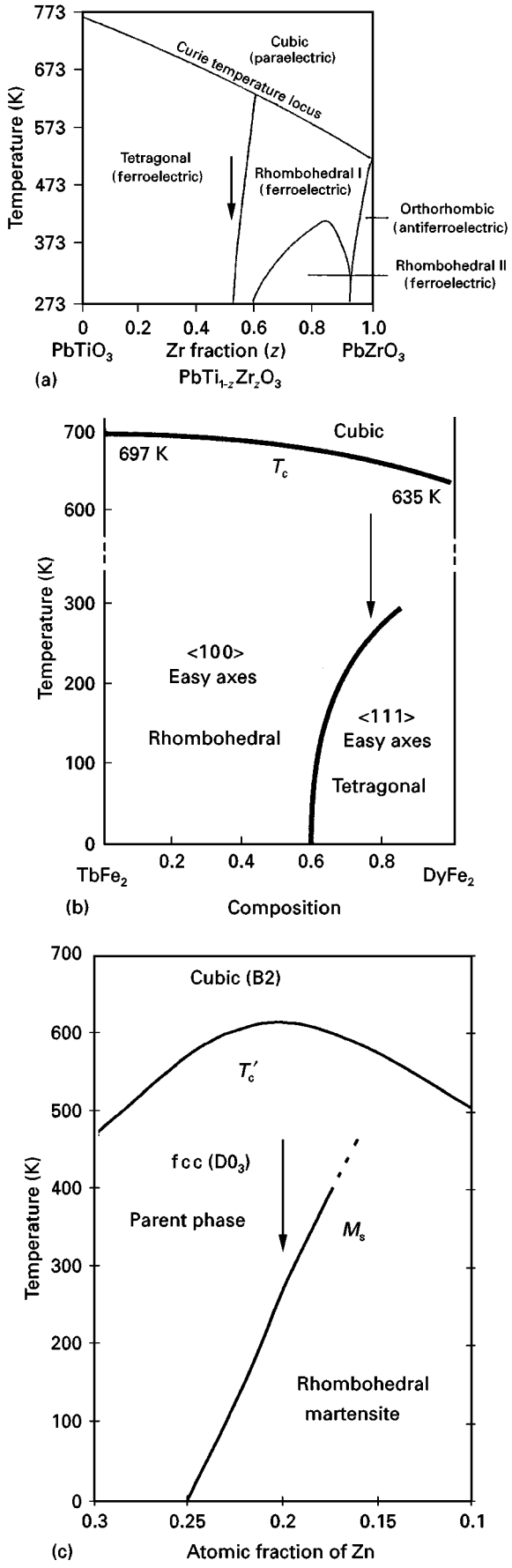

Figure 5 Phase diagrams of three prototypes of smart materials showing some common features. (a) Piezoelectric Pb(Zr, Ti) O_3 [212], (b) magnetostrictive (Tb, Dy) Fe_2 [176], and (c) ferroelastic Cu–*x*Zn–10 at % Al shape-memory alloy (only a portion of metastable phase diagram of interest is shown, estimated from a modified Bragg–Williams model). The arrows indicate the morphotropic phase boundaries and the compositions of the materials in practical use.

proper stresses are applied at temperatures near the parent–martensitic phase boundary. Experimentally, it has been verified that both uniaxial tensile and compressive stresses increase the martensitic transformation temperature, M_s, without regard to the sense of external stresses and the kind of alloy systems [179–181]. The critical stress, (σ_τ), to induce the martensitic transformation at a given temperature is guided by the well-known Clausius–Clapeyon equation

$$\frac{d\sigma_\tau}{dT} = \frac{\Delta H}{V T_0 \Delta\varepsilon} \tag{4}$$

where ΔH is the transformation enthalpy, $\Delta\varepsilon$ the transformation strain, V the molar volume and T_0 is the temperature at which the parent and martensite phases are in equilibrium at zero stress. Generally, the value of σ_τ increases linearly with increasing temperature. Fig. 6 shows the stress–strain curves at different temperatures for a Ti–Ni SMA and Ce-TZP SMM. More systematic descriptions of the stress–strain–temperature space can be demonstrated by the well-established constitutive relations [182–186]. The most simple form of the one-dimensional SMA constitutive equation is given by

$$\sigma - \sigma_0 = D(\varepsilon - \varepsilon_0) + \Theta(T - T_0) + \Omega(\xi - \xi_0) \tag{5}$$

where D is Young's modulus, Θ is the thermoelastic tensor, Ω is the transformation tensor, and σ, ε and T are the state variables for stress, strain and temperature, respectively. $\xi(\sigma, T)$ is the martensitic fraction. The stress-induced martensitic transformations in most SMAs (excluding some iron-based alloys) are reversible when unloading, giving rise to a mechanical shape memory: this effect is usually called pseudoelasticity. More importantly, the recoverable transformation strain for most polycrystalline SMAs can be as much as up to 8%, for some single-crystalline SMAs may exceed 10% [13, 14, 18], resulting in a very high elastic energy storage capacity.

The martensite phase consists of highly twinned polydomains (martensite variants). There are 24 possible kinds of martensite variants in SMAs. The crystallographic characteristics can be well described by the phenomenological crystallographic theory of martensitic transformations [13]. When subjecting the material in the matensite state to an applied stress, the variants undergo a self-accommodating pattern of shear-induced shrinkage, growth and reorientation by detwinning, resulting in twin-induced inelastic strains which can be described by some simple relations, as established by Roytburd [187, 188]. Unloading from the inelastic state may leave a residual strain, but it can be recovered by heating the material to the parent phase. This is the so-called shape-memory effect (SME). The mechanism of the shape-memory effect was overviewed in more detail by Miyazaki and Otsuka [13]. Besides the unique behaviour, heat-induced formation of the parent phase generates a considerable recovery stress, which can be used for mechanical actuation. The recovery stress is a function of prestrain and temperature (i.e. the volume fraction of

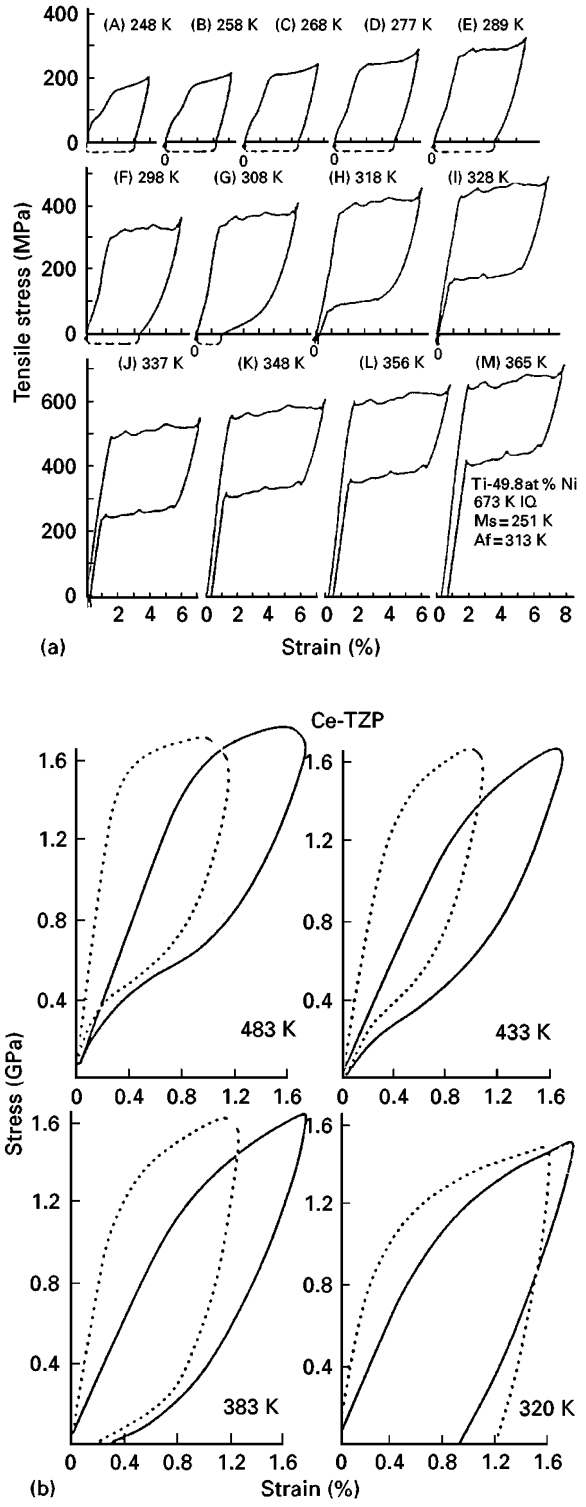

Figure 6 Typical stress–strain curves at various temperatures for shape-memory materials. (a) A Ti–49.8 at % Ni shape-memory alloy [13]; (b) a CeO_2-stabilized tetragonal zirconia polycrystal (Ce-TZP) shape-memory ceramic [127] (—) axial, (---) radial. In both the materials the critical stress to induce the transformation shows a remarkable increase with increasing temperature.

transformed phase), and can be experimentally determined or theoretically estimated from the constitutive relations [182–186]. Fig. 7 shows the measured recovery stress as a function of temperature for a Ti–Ni alloy for different prestrains. Through thermomechanical training, both one-way SME and two-way SME can be achieved. These characteristics of SMAs can be applied for actuation, shape or position

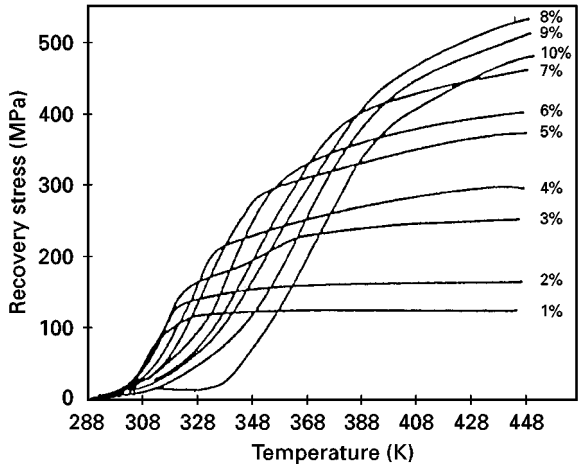

Figure 7 Recovery stress as a function of temperature and prestrain for a binary Ti–Ni shape-memory alloy [20].

control, impact or creep resistance and energy conversion.

From a thermodynamic point of view, pressure, like temperature, is an independent variable that can change the free energy and thus phase state of a material. It is well known that the Gibbs' chemical free energy, G, is defined as

$$G = H - TS \tag{6}$$

where T is temperature, H and S are the enthalpy and entropy of the system, respectively. Based on the first and second laws of thermodynamics, it can be easily derived that

$$\mathrm{d}G = V\mathrm{d}P - S\mathrm{d}T \tag{7}$$

where P is pressure and V is volume. It is evident that the free energy can be altered by varying either pressure or temperature. At a given temperature, the increase in pressure will increase the free energy of the system. As a consequence, the system will tend to transform into other phases that have a lower free energy under the pressure, or, to decrease its volume through contraction, which will change the electronic structures and in turn the physical properties, and thermodynamic state of the material. Pressure-induced phase transitions have been observed in a very wide range of materials. Of particular interest are the reversible pressure-induced transitions, which may implicate shape-memory effect. More recently, a memory glass exhibiting structural reversibility has been discovered by Kruger and Jeanloz [189]. At 300 K, both polycrystalline and single-crystal $AlPO_4$ berlinite became amorphous when the pressure was increased above 15 GPa. On reducing the pressure below 5 GPa, they reconverted from the glassy state to the crystalline state with the same orientation as the original crystal, implying a memory capacity of the crystallographic structure. Similar phase transitions have been observed in $GaAsO_4$ and other quartz-like structure [190, 191].

The effects of hydrostatic pressure on martensitic transformations in some shape-memory alloys, including Cu–Al–Ni, Ti–Ni, Fe–Pt, Fe–Ni, Fe–Ni–C, Fe–Ni–Mn and Fe–Ni–Co–Ti alloys have been

systematically investigated by Kakeshita and coworkers [192]. The M_s temperature may be increased or decreased with increasing hydrostatic pressure, depending upon the volume change associated with the martensitic transformation. If volume contraction occurs in the transformation, as in Cu–Al–Ni, Ti–Ni and some iron-based alloys exhibiting thermoelastic transformations, static pressures can induce the martensitic transformation, and the M_s temperature increases linearly with increasing pressure. On the other hand, in ferrous alloys exhibiting non-thermoelastic transformation, hydrostatic pressures decrease M_s temperature due to the volume expansion associated with the transformation. Because the Invar effect introduces additional volume changes in some ferrous Invar alloys, the effects of static pressure on the martensitic transformation are affected by the Invar effect. Although the pressure-induced martensite is defined as "stress-assisted" martensite, the morphology is, however, very similar to that of thermally induced ones [192].

Martensitic transformations can also be induced by dynamic pressures generated by intense shock waves. A well-known example is that oriented graphite will undergo a martensitic transformation to form diamond under shock compression [193]. Shock-induced martensites have been observed in Ti–Ni SMAs, Fe–Mn, Fe–Ni, Fe–Ni–C and other kinds of steel [194–197].

3.3. Magnetic field-induced transformations

In some β-phase and iron-based shape-memory alloys, the paramagnetic–ferromagnetic transitions or magnetic ordering transitions occur at temperatures above the start points of martensitic transformations. In these alloys, the martensitic transformations may be induced by applying magnetic fields. The effects of magnetic fields on the martensitic transformations in some ferrous alloys and steels have been extensively investigated [198–204]. It has been established that the critical magnetic field for inducing martensites and the transformation start temperature obey to the following equation [202]

$$\Delta G(M_s) - \Delta G(T) = -\Delta M(T)H - \frac{1}{2}\chi_h^p H^2 + \varepsilon\frac{\partial\omega}{\partial H}HB \quad (8)$$

where $\Delta G(M_s)$ and $\Delta G(T)$ represent the difference in Gibbs' chemical free energy between the austenite and martensite phases at M_s and T temperatures, respectively. $\Delta M(T)$ the difference in spontaneous magnetization between the austenitic and martensitic states at T, H the magnetic field, χ_h^p the high magnetic field susceptibility in the austenite phase, ε_0 the transformation strain, ω the forced volume magnetostriction and B the austenitic bulk modulus. The first, second and third terms on the right-hand side of Equation 8 represent the energies due to the magnetostatic, high-field susceptibility and forced volume magnetostriction effects, respectively [202]. Generally, a large difference in magnetic moment between parent and martensite phases facilitates the field-induced transformation, and vice versa. It has been found that the martensitic transformations in Ti–Ni and Cu–Al–Ni shape-memory alloys are not affected by magnetic field because of their small difference in the magnetic moment between the parent and martensite phases [202]. However, Kakeshita *et al.* [203] found a magnetoelastic martensitic transformation in an ausaged Fe–Ni–Co–Ti SMA. In the alloy, the martensites are induced when a magnetic field is applied and revert to the parent phase once the magnetic field is removed. This kind of shape-memory alloy may be utilized as a magnetically sensitive device as well as a thermally sensitive one [202].

If the martensites are ferromagnetic, there also exists the possibility of rearranging the martensite variants by applying a magnetic field. Because the spontaneous strain in martensitic materials is commonly one order of magnitude larger than that of giant magnetostrictive materials, the field-induced strain available from the materials is potentially much larger than giant magnetostrictive materials [205–207]. Fig. 8 schematically illustrates the magnetic field-induced deformation process in comparison with the stress-induced martensite detwinning and electric-field deformation processes. In the ferromagnetic martensite, the magnetization vectors are aligned to the easy magnetization direction in each twin variant. When an external magnetic field is applied, the magnetization vectors will tend to turn parallel to the direction of the external magnetic field. If the martensite has a large saturation magnetization and a favourable anisotropy and the energy for twin-boundary motion is low, which can guarantee some easy crystallographic axes and low energy transformation paths, then the twin variant will reorientate in the same way as in the stress-induced detwinning. In certain conditions, the twin boundaries will move back when the external field is switched off or a reverse field is applied, resulting in "magnetoelasticity" and "magnetosuperelasticity" [205–211].

Experimentally, James and Wuttig [207] and Ullakko *et al.* [208, 209] have evinced the field-generated movement of martensite domains and the remarkable change of volume fractions in several ferromagnetic alloys. Fig. 9 shows that for $Fe_{70}Pd_{30}$ single crystals at modest fields with a two-field arrangement, strains of up to 0.6% were obtained by applying a transverse field parallel to [0, 0.95, 0.31] at 256 K, with a fixed axial field of 2300 Oe [207]. Meanwhile, the field-induced strains of nearly up to 0.2% along [0 0 1] in unstressed crystals of the Heusler alloy Ni_2MnGa with magnetic fields of 8 kOe at 265 K were demonstrated [208]. The low level of strains was due to the fact that only a small fraction of variants was rearranged by the field. To achieve larger strains, the magnetization energy and the anisotropy should be sufficient and favourable to induce the motion of all the twin boundaries.

3.4. Electric field-induced transformations

At ambient temperatures, the perovskites may have either a ferroelectric or an antiferroelectric phase with

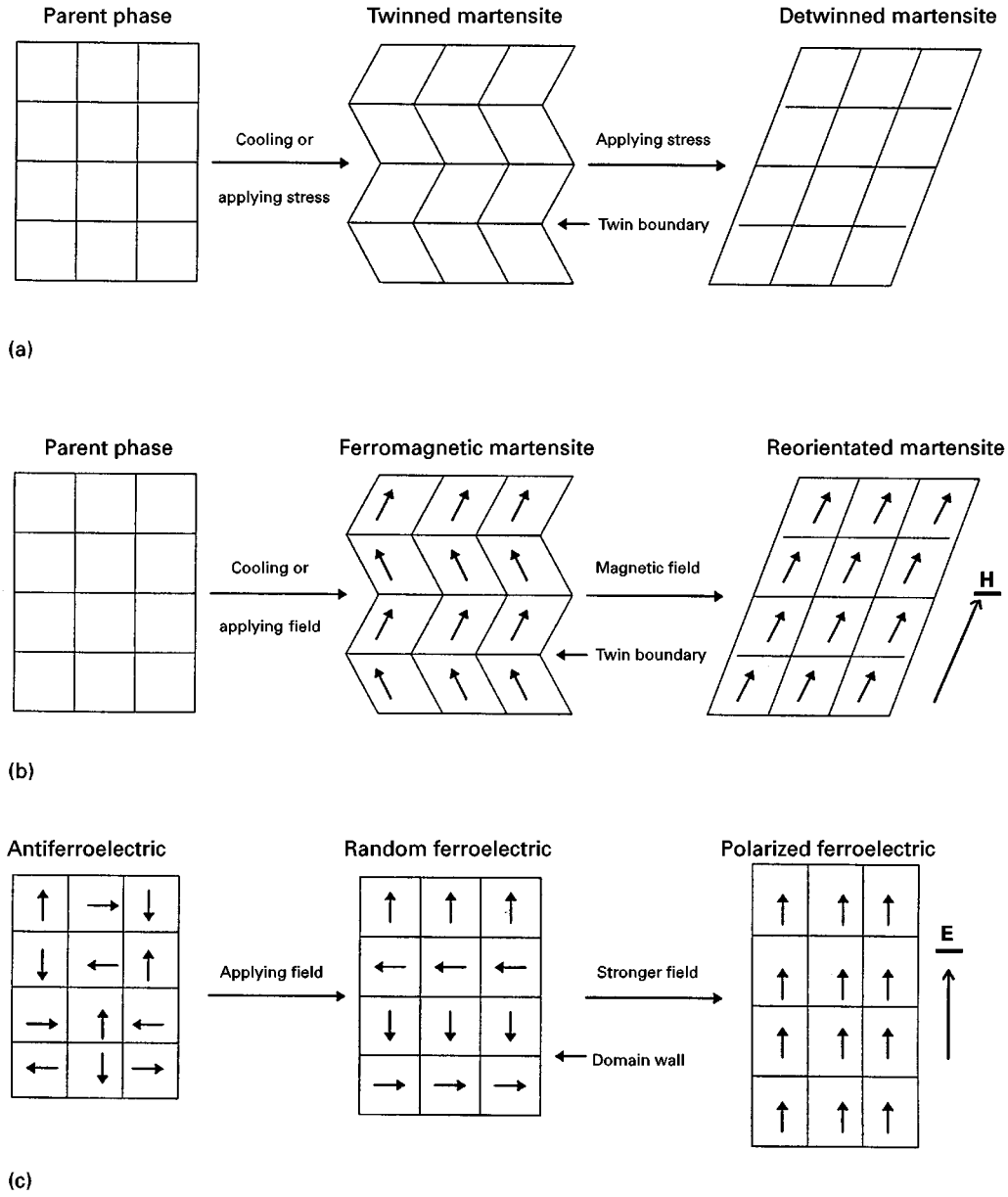

Figure 8 Schematic illustration of the deformation processes in the ferroelastic, ferromagnetic, and ferroelectric materials. (a) Stress-induced martensitic transformation by twinning and reorientation of martensite domains by detwinning, (b) magnetic field-induced transformation and reorientation of magnetic domains, (c) electric field-induced AFE–FE transformation and polarization of FE.

rhombohedral or tetragonal structure [175, 212]. As mentioned above, the compositions of the ferroelectric shape-memory ceramics are usually so selected that the ceramics have an antiferroelectric structure but they are close to the ferroelectric phase boundary, as shown in Fig. 10. In this region, the antiferroelectric can be transformed into the ferroelectric at high electric fields. Both the metastable AFE and FE phases may coexist, rendering the forward switching AFE–FE under increasing field and the backward switching FE–AFE under decreasing field. The phase stability of the phases can be predicted based on a thermodynamic model [145]. The transformations can also be approached within the "constrained theory" established by James and Wuttig for ferromagnetics [207]. Because antiferroelectrics do not display any macroscopic polarization and very little strain is achieved when applied at low electric fields, the AFE–FE transformation and the subsequent poling of the ferroelectric domains will cause mechanical strains, as illustrated in Fig. 8c. Suppose the magnitude of the sublattice polarization remains essentially unchanged during the transformation, then, according to the two-sublattice model [146, 150], the spontaneous strain associated with field-induced paraelectric–ferroelectric (PE-FE) transition is described by

$$\varepsilon_{P-F} = QP_1^2 \tag{9}$$

while the spontaneous strain in the antiferroelectric state, ε_{AFE}, and the strain in the ferroelectric state induced from the antiferroelectric by applying a field, ε_{FE}, can be expressed, respectively, as

$$\varepsilon_{AFE} = Q(1 - \Omega)P_A^2 \tag{10}$$

$$\varepsilon_{FE} = Q(1 + \Omega)P_F^2 \tag{11}$$

where P_A and P_F are two-sublattice based polarizations, P_r is the field-induced polarization, Q and Ω are

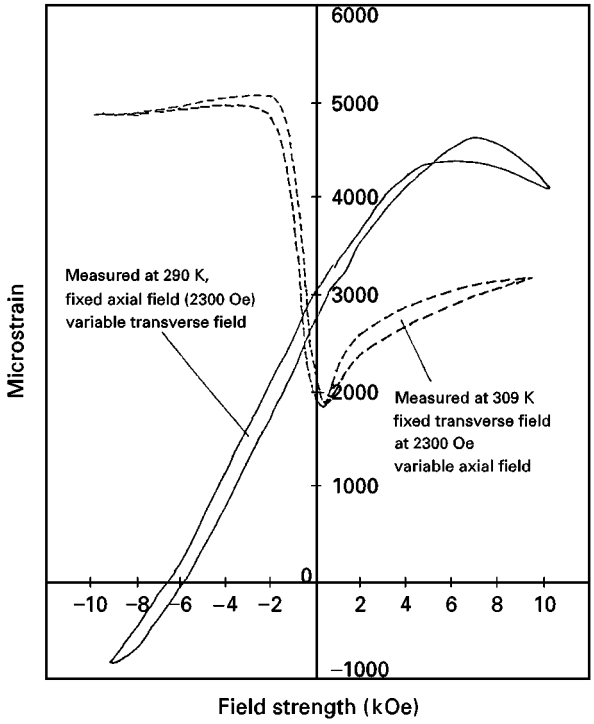

Figure 9 Magnetic field-induced strains in a $Fe_{70}Pd_{30}$ single-crystal shape-memory alloy with two-field arrangements. The solid lines were measured at 290 K, with a fixed axial field at 2300 Oe and variable transverse field, no stress was applied. (- - -) Measured at 309 K, with a fixed transverse field at 2300 Oe and variable axial field, no stress was applied [207].

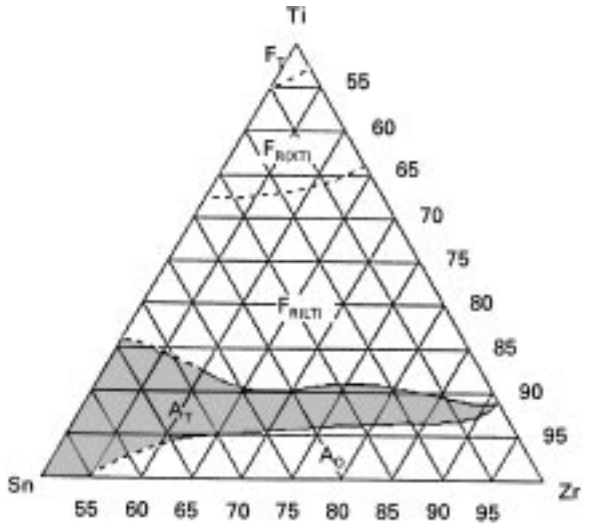

Figure 10 Phase diagram for $Pb_{0.97}La_{0.02}(ZrTiSn)O_3$ shape-memory ceramics [147, 150]. The shadowed area indicates the composition range wherein the antiferroelectric–ferroelectric transition can be induced by applying a field.

the electrostrictive coefficients. Because, $P_A^2 = P_F^2$, the total field-induced strains in an antiferroelectric crystal, ε_{A-F}, can be estimated as

$$\begin{aligned}\varepsilon_{A-F} &= \varepsilon_{FE} - \varepsilon_{AFE} \\ &= 2Q\Omega P_F^2 \\ &= Q\Omega P_1^2 \end{aligned} \quad (12)$$

By comparing Equations 9 and 12, it is evident that the strain is larger if the ferroelectric polarization is

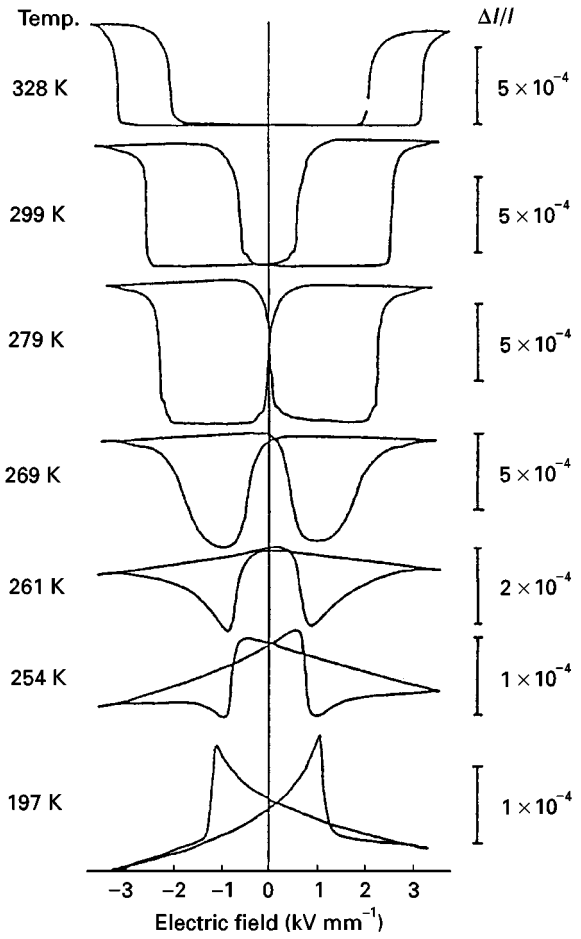

Figure 11 Electric field-induced transverse elastic strains at various temperatures for the $Pb_{0.99}Nb_{0.02}((Zr_{0.6}Sn_{0.4})_{0.94}Ti_{0.06})_{0.98}O_3$ shape-memory ceramic [146].

induced from an antiferroelectric state than if it is induced from a paraelectric state because $\Omega > 1$ [150]. Besides composition and field strength, the field-induced strains show a strong temperature dependence which can be described by the modified Clausius–Claperon relation [145]

$$\frac{dE}{dT} = -\frac{\Delta H}{T\Delta P} \quad (13)$$

where E is the field strength, T the temperature, ΔH and ΔP are the enthalpy and polarization change at the AFE–FE transitions, respectively. In addition, other factors such as pressure, stress and the frequency of the electric field also affect the transformation and the field-induced strains [142, 146, 147, 150]. Systematic descriptions of the static and dynamic responses of the material can be approached by employing phenomenological models based on rate laws [148]. Fig. 11 shows the transverse elastic strains induced by field at various temperatures in a $Pb_{0.99}Nb_{0.02}((Zr_{0.6}Sn_{0.4})_{1-y}Ti_y)_{0.98}O_3$ ($y = 0.06$) ceramic.

Some phase transformations in polymers, gels or inorganic substances can be activated by certain chemical stimuli, resulting in so-called chemostrictive effects which may implicate shape-memory capacity. Further information on the phase transitions can be found in some recent reviews [168, 169, 175].

4. Inherent functions and adaptive properties

The phase transformations in the shape-memory materials are accompained by remarkable or even drastic changes in the physical and mechanical properties, such as yield stress, elastic modulus, hardness, damping, shape recovery, thermal conductivity, thermal expansion coefficient, resistivity, magnetic susceptibility, flexibility, vapour permeability, shape fixity and dielectric constant, enabling the materials to exhibit some novel functions or making them adaptable to the external changes in temperature, stress, magnetic or electrical field. In general, the following features or inherent primitive intelligence of shape-memory materials may be utilized in various envisaged engineering approaches for smart systems:

1. sensing – SMMs are sensitive to some environmental changes such as thermal, stress, magnetic or electric field stimuli;
2. switch or control capacity – the environmental stimulus must reach to a critical value to trigger the operation;
3. actuation – SMMs can provide very large displacements (superelasticity or pseudoelasticity) and huge forces for actuation;
4. adaptivity – various properties show remarkable changes due to phase transformations;
5. memory and recovery – the shape or other changes are reversible and can be repeated;
6. energy storage and conversion – a considerable amount of energy can be stored, and thermal–mechanical, chemical–mechanical, magnetic–mechanical and electric–mechanical energy conversions may be achieved;
7. damping – most SMMs have high inherent specific damping capacity due to the characteristic microstructures and phase transitions.

Table I summarizes some typical properties of binary Ti–Ni shape-memory alloys, in the martensite and parent-phase state. Because the properties are sensitive to the alloy composition, processing parameters, testing methods and conditions, the recorded data of the SMAs are largely scattered. The values given in Table I are based on the report by Jackson *et al.* [20], but modified according to the numerous data resources obtained by various researchers during recent years. The changes in the properties can be utilized to achieve some adaptive functions such as self-strengthening, self-relaxation or self-healing in engineering structures. By incorporating the SMMs with other functional materials or structural materials, it is possible to tune or tailor the static and dynamic properties of the composites and structures. The engineering approaches in this area will be described in the following paper [213].

TABLE I Some typical properties of binary Ti–Ni shape-memory alloys

Melting point	$\sim 1573\,K$
Density	$6.4–6.5\,g\,cm^{-3}$
Transformation temperatures	173–390 K
Transformation enthalpy	$1.46–1.88\,kJ\,mol^{-1}$
Transformation hysteresis	20–50
Recoverable strain	
one-way-effect	$< 8\%$
two-way-effect	$< 5\%$
Recovery stress	$< 500\,MPa$
Damping capacity, Q^{-1}	$\sim 10^{-2}$
Ultimate tensile strength	800–1100 MPa
Yield strength	
Parent phase	200–800 MPa
Martensite	70–200 MPa
Young's modulus	
Parent phase	50–90 GPa
Martensite	10–35 GPa
Shear modulus	
Parent phase	15–20 GPa
Martensite	3.5–5 GPa
Thermal expansion coefficient	
Parent phase	$10.0–11.0 \times 10^{-6}\,K^{-1}$
Martensite	$5.8–8.6 \times 10^{-6}\,K^{-1}$
Thermal conductivity	
Parent phase	$0.18\,W\,cm^{-1}\,K^{-1}$
Martensite	$0.086\,W\,cm^{-1}\,K^{-1}$
Electrical resistivity	
Parent phase	$70–110\,\mu\Omega\,cm$
Martensite	$40–70\,\mu\Omega\,cm$
Magnetic susceptibility	
Parent phase	$2.7–3.0 \times 10^{-6}$ e.m.u. g^{-1}
Martensite	$1.9–2.1 \times 10^{-6}$ e.m.u. g^{-1}

5. Technical challenges and perspectives

Table II compares some selective features of shape-memory material (Ti–Ni SMA), piezoelectric ceramic (PZT) and magnetostrictive material (Terfenol-D). Among the smart materials, SMAs have the largest output energy density, and can provide the greatest displacements or strokes. However, shape-memory materials do have some shortcomings to be overcome before their engineering significance is more widely recognized in the industrial world. The problems addressed range from fundamental to engineering aspects: fabrication and processing of demanding high-quality and low-cost materials; precise prediction and modelling of the material behaviour and optimal design; controlling the microstructures and, above all, tailoring some crucial technical parameters such as characteristic transformation temperatures within desirable range; clear understanding of the origins of such issues as hysteresis, phase instabilities and ageing effects, degradation and fatigue, etc. In addition to the efforts to improve the even commercial materials, new shape-memory materials with higher technical quality should be designed and developed to meet the increasing demand of the Hi-tech society. Of particular technical significance are new shape-memory materials that can provide large displacements, huge stresses and exhibit superior dynamic response. This can be approached in two ways. The first route is to incorporate SMMs with other structural or functional materials to form hybrid composites which will benefit from individual component materials, thereby achieving compromised but optimized overall performance of the component materials system. For instance, the main disadvantages of SMAs are their insuperior dynamic response and low efficiency. Meanwhile, the

TABLE II Comparison of characteristics of shape-memory alloys, piezoelectric ceramics and magnetostrictive materials as actuation materials

Properties	Shape-memory alloy (Ti–Ni)	Piezoelectric (PZT)	Magnetostrictive (Terfenol-D)
Compressive stress (MPa)	~800	60	700
Tensile strength (MPa)	800–1000	30–55	28–35
Young's modulus (GPa)	50–90 (P)	60–90 (Y^E)[a]	25–35 (Y^H)[c]
	10–35 (M)	~110 (Y^D)[b]	50–55 (Y^B)[d]
Maximum strain	~0.1	~0.001	~0.01
Frequency (Hz)	0–100	1–20 000	1–10 000
Coupling coefficient	~	0.75	0.75
Efficiency (%)	3–5	50	80
Energy density ($kJ\,m^{-3}$)	300–600	~1.0	14–25

[a] modulus for constant electric field
[b] modulus for constant electric displacement
[c] modulus for constant magnetizing field
[d] modulus for constant induction field

conventional piezoelectric or electrostrictive ceramics have a superior dynamic response but their displacements are quite small and most of them are very brittle. Combining SMAs with piezoelectric or magnetostrictive materials, field-activated smart composites can be designed, which may generate a larger displacement than conventional piezoelectric ceramics or magnetostrictive materials and have an improved dynamic response as compared to monolithic SMAs. More recently, some pioneers have explored the technical feasibility of smart thin-film heterostructures by depositing the SMA thin films on piezoelectric or magnetostrictive substrates. However, the complexity of the fabrication processing and the interface bonding and dynamic coupling of dissimilar components remain tough issues for the composites [213].

The alternative is to improve the monolithic shape-memory materials by employing new processing techniques or to design a new generation of shape-memory materials. The development of deposited thin-film shape-memory alloys, as we described above, is one of the efforts directed to this objective. Also worth mention are the recently developed porous shape-memory alloys [214, 215]. Bulk Ti–Ni alloys with different porosity, exhibiting superelasticity and shape-memory effect, have been successfully manufactured via the powder metallurgical route. The porous SMAs are very desirable for some biomedical applications because the alloys have good biocompatibility and their porous structure favours in-growth of living tissues and firm fixation. Naturally, it reminds us of bone – a typical biomimetic model. Bone is also porous; moreover, it exhibits pyroelectricity and piezoelectricity, and maintains the skeletal homeostasis and mineral homeostasis for the body [1]. After the model, biomimetic artificial bone materials based on the porous SMAs and other advanced materials may be developed. For instance, microballoons or microtubes coated by some functional material layers can be constructed in the porous SMAs which may provide a suitable substrate or skeleton to grow heterostructures with certain intelligence.

In principle, the deformation of the polydomains in the ferromagnetic and ferroelectric materials by applying external fields can be controlled just the same way as the stress-induced deformation of the martensites in ferroelastic SMAs. The next challenging objective, therefore, is to explore new potentially commercial materials wherein the martensitic-like transformations and the reorientation of the domains can be induced by magnetic fields or electric fields at ambient temperatures. The design concepts and strategies for finding new ferromagnetic and ferroelectric shape-memory materials have been proposed [142, 205–211]. In this aspect, the remarked common features shared by several smart material systems, and the successful development story of the giant magnetostrictive materials Terfenol-D [176, 216–218] may offer some clues or inspirations.

Acknowledgements

The authors thank Prof. J. Van Humbeeck of K. U. Leuven and Mr J. Cederstrom, Scandinavian Memory Metals, AB, for critical reading of the manuscript, Professor R. D. James, University of Minnesota, and Professor D. S. Grummon, Michigan State University, for providing their papers prior to publication. One of the authors (Z G W) wishes to acknowledge the Royal Institute of Technology (KTH) for offer of a fellowship to work at KTH.

References

1. M. V. GANDHI and B. S. THOMPSON, "Smart Materials and Structures" (Chapman & Hall, New York, 1992).
2. T. TAKAGIL, *J. Intelligent Mater. System Struct.* **1** (1990) 149.
3. *Idem*, in "Proceedings of the 3rd International Conference on Intelligent Materials", edited by P. F. Gobin and J. Tatibouet (Technomic, Lancaster, 1996) p. 2.
4. C. A. JAEGER and C. A. ROGERS, in "Proceedings of the ARO Workshop on Smart Materials, Structures and Mathematical Issues", edited by C. A. Rogers (ARO, Washington, 1988) p. 14.
5. S. NOZAKI and K. TAKAHASHI, in "Proceedings of the 2nd International Conference on Intelligent Materials", edited by C. A. Rogers and G. G. Wallace (Technomic, Lancaster, 1994) p. 1230.
6. G. BECK and P. F. GOBIN, in "Proceedings of the 1st International Conference on Intelligent Materials", edited by T. Takagi, K. Takahashi, M. Aizawa and S. Miyata (Technomic, Lancaster, 1992) p. 9.

7. F. MUCKLICH and H. JANOCHA, *Z. Metallkde* **87** (1996) 357.
8. C. A. ROGERS, *J. Intelligent Mater. System Struct.* **4** (1993) 4.
9. M. SHAHINPOOR, "Smart Structures and Materials 1996: Smart Materials Technologies and Biomimietics", Vol. 2716 (SPIE, Bellingham, 1996) p. 238.
10. H. B. STROCK, *Am. Ceram. Soc. Bull.* 75 (4) (1996) 71.
11. W. B. SPILLMAN Jr, J. S. SIRKIS and P. T. GARDINER, *Smart Mater. Struct.* **5** (1996) 247.
12. W. J. BUEHLER, J. V. GILFRICH and K. C. WEILEY, *J. Appl. Phys.* **34** (1963) 1467.
13. S. MIYAZAKI and K. OTSUKA, *ISIJ Int.* **29** (1989) 353.
14. H. FUNAKUBO (ed.), 'Shape Memory Alloys" (Gordon and Breach Science, New York, 1984).
15. T. W. DUERIG, K. N. MELTON, D. STÖCKEL and C. M. WAYMAN (eds), "Engineering Aspects of Shape Memory Alloys", (Butterworth-Heinemann, London, 1990).
16. Y. CHU and H. TU (eds), "Shape Memory Materials' 94" (International Academic, Beijing, 1994).
17. A. R. PELTON, D. HODGSON and T. DUERIG (eds), "Shape Memory and Superelastic Technologies" (SMST, Pacific Grove, CA, 1994, 1997).
18. For example, "Proceedings of International Conference on Martensitic Transformations", (Switzerland, 1995), (USA, 1992), (Australia, 1989), (Japan, 1986), etc..
19. C. M. WAYMAN, *Progr. Mater. Sci.* **36** (1992) 203.
20. C. M. JACKSON, H. J. WAGNER and R. J. WASILEWSKI, "55-Nitinol–The Alloy With a Memory: Its Physical Metallurgy, Properties, and Applications: A Report" (NASA Washington, 1972).
21. D. E. HODGSON, M. H. WU and R. J. BIERMANN, "Shape Memory alloys" (Shape Memory Applications, Inc., Santa Clara, 1995).
22. T. W. DUERIG and A. R. PELTON, "Materials Properties Handbook: Titanium Alloys" (ASM, Metals Park, 1994) p. 1035.
23. R. STALMANS and J. VAN HUMBEECK, "Shape Memory Alloys: Functional and Smart" (Katholieke Universiteit Leuven, Leuven, 1996).
24. T. H. NAM, T. SABURI and K. SHIMIZU, *Mater. Trans. JIM* **32** (1990) 959.
25. T. H. NAM, T. SABURI, Y. NAKATA and K. SHIMIZU, *ibid.* **31** (1990) 1050.
26. K. OTSUKA, in "Shape Memory Materials' 94", edited by Y. Chu and H. Tu, (International Academic, Beijing, 1994) p. 129.
27. W. J. MOBERLY and K. N. MELTON, in "Engineering Aspects of Shape Memory Alloys", edited by T. W. Duerig, K. N. Melton, D. Stöckel and C. M. Wayman (Butterworth-Heinemann, London, 1990) p. 46.
28. K. N. MELTON, *ibid.*, p. 21.
29. T. W. DUERIG, K. N. MELTON and J. L. PROFT, *ibid.*, p. 130.
30. M. PIAO, S. MIYAZAKI, K. OTSUKA and N. NISHIDA, *Mater. Trans. JIM* **33** (1992) 337.
31. *Idem*, *ibid.* **33** (1992) 346.
32. C. S. ZHANG, L. C. ZHAO, T. W. DUERIG and C. M. WAYMAN, *Scripta Metall. Mater.* **24** (1990) 1807.
33. P. G. LINDQUIST and C. M. WAYMAN, in "Engineering Aspects of Shape Memory Alloys", edited by T. W. Duerig, K. N. Melton, D. Stöckel and C. M. Wayman (Butterworth-Heinemann, London, 1990) p. 58.
34. J. BEYERS and J. H. MULDER, *Mater. Res. Soc. Symp. Proc.* **360** (1995) 443.
35. S. M. RUSSELL and F. SCZERZENIE, *ibid.*, p. 455.
36. S. M. TUOMINEN, in "Proceedings of the 1st International Conference on Shape Memory and Superelastic Technologies", edited by A. R. Pelton, D. Hodgson and T. Duerig, (SMST, Fremont, 1994) p. 49.
37. J. H. MULDER, J. BEYER, P. DONNER and J. PETERSEIM, *ibid.*, p. 55.
38. S. K. WU and Y. C. LO, *Mater. Sci. Forum* **56–68** (1990) 619.
39. M. H. WU, in "Engineering Aspects of Shape Memory Alloys", edited by T. W. Duerig, K. N. Melton, D. Stöckel and C. M. Wayman (Butterworth-Heinemann, London, 1990) p. 69.
40. D. Z. YANG and Z. G. WEI, in "Shape Memory Materials' 94", edited by Y. Chu and H. Tu (International Academic, Beijing, 1994) p. 319.
41. D. P. DUNNE and N. F. KENNON, *Metals Forum* **4** (1981) 176.
42. M. A. MORRIS, *Acta Metall. Mater.* **40** (1992) 1573.
43. Z. G. WEI, H. Y. PENG, W. ZOU and D. Z. YANG, *Metall. Mater. Trans.* **28A** (1997) 955.
44. K. SUGIMOTO, K. KAMEI and M. NAKANIWA, in "Engineering Aspects of Shape Memory Alloys", edited by T. W. Duerig, K. N. Melton, D. Stöckel and C. M. Wayman (Butterworth-Heinemann, London, 1990) p. 89.
45. J. VAN HUMBEECK, in "Proceedings of the 3rd International Conference on Intelligent Materials", edited by P. F. Gobin and J. Tatibouet (Technomic, Lancaster, 1996) p. 442.
46. S. MIYAZAKI, "Shape Memory Alloys", (Springer, Vienna, New York, 1996) p. 69.
47. J. VAN HUMBEECK and J. CEDESTROM, in "Proceedings of the 1st International Conference on Shape Memory and Superelastic Technologies", edited by A. R. Pelton, D. Hodgson and T. Duerig, (SMST, Fremont, 1994) p. 1.
48. T. MAKI, *Mater. Sci. Forum* **56–58** (1990) 156.
49. R. KAINUMA, N. ONO and K. ISHIDA, *Mater. Res. Soc. Symp. Proc.* **360** (1995) 467.
50. E. P. GEORGE, C. T. LIU, J. A. HORTON, C. J. SPARKS, M. KAO, H. KUNSMANA and T. KING, *Mater. Charact.* **32** (1994) 139.
51. R. KAINUMA, K. ISHIDA and T. NISHIZAWA, *Metall. Trans.* **23A** (1992) 1447.
52. V. A. CHERNENKO and V. V. KOKORIN, in "Proceedings of the International Conference on Martensitic Transformations' 92", edited by C. M. Wayman and J. Perkins (Monterey Inst. of Advanced Studies, Monterey, 1993) p. 1205.
53. Y. N. KOVAL, G. S. FIRSTOV, J. VAN HUMBEECK, L. DELAEY and W. Y. JANG, *J. Phys. IV* **C8** (1995) 1103.
54. C. Y. LEI, J. S. LEE PARK, H. R. P. INOUE, C. M. WAYMAN, in "Proceedings of the International Conference on Martensitic Transformations' 92", edited by C. M. Wayman and J. Perkins (Monterey Inst. of Advanced Studies, Monterey, 1993) p. 539.
55. J. S. LEE PARK, C. Y. LEI, M. H. WU, H. R. P. INOUE, C. M. WAYMAN, *ibid.*, p. 533.
56. M. R. IBARRA, T. S. CHIEN and A. S. PAVLOVIC, *J. Less-Common Metals* **153** (1989) 233.
57. A. P. JARDINE, J. S. MADSEN and P. G. MERCADO, *Mater. Charact.* **32** (1994) 169.
58. A. P. JARDINE, *Mater. Res. Soc. Symp. Proc.* **276** (1992) 31.
59. A. D. JOHNSON, J. D. BUSCH, C. A. RAY and C. SLOAN, *ibid.* **276** (1992) 151.
60. A. D. JOHNSON, J. D. BUSCH, in "Proceedings of the 1st International Conference on Shape Memory and Superelastic Technologies", edited by A. R. Pelton, D. Hodgson and T. Duerig, (SMST, Fremont, 1994) p. 299.
61. P. KRULEVITCH, A. P. LEE, P. B. RAMSEY, J. C. TREVINO, J. HAMILTON and M. A. NORTHRUP, *J. Microelectromech. Systems* **5** (1996) 270.
62. A. P. JARDINE, *Mater. Res. Soc. Symp. Proc.* **246** (1992) 427.
63. Q. SU, T. KIM, Y. ZHENG and M. WUTTIG, "Smart Structures and Materials 1995: Smart Materials", Vol. 2441 (SPIE, Bellingham, 1995) p. 179.
64. A. P. JARDINE, *Smart Mater. Struct.* **3** (1994) 140.
65. H. ANDOH, T. MINEMURA, I. IKUTA and Y. KITA, *J. Jpn Inst. Metals* **50** (1986) 430.
66. J. A. WALKER, K. J. GABRIEL and M. MEHREGANY, *Sensors and Actuators* **A21-A23** (1990) 243.
67. J. D. BUSCH, A. D. JOHNSON, C. H. LEE and D. A. STEVENSON, *J. Appl. Phys.* **68** (1990) 6224.
68. A. D. JOHNSON, *J. Micromech Microeng.* **1** (1991) 34.
69. K. IKUTA, in "Proceedings of the IEEE International Conference Robotics and Actuation", (IEEE, Los Alamitos, 1990) p. 2156.
70. K. IKUTA, H. FIJITA, M. IKEDA and S. YAMASHITA, in "Proceedings of the IEEE Micro-Electro-Mechanical Systems", (IEEE, Napa Valley, 1990) p. 38.

71. K. KURIBAYASHI and M. YOSHITAKE, *ibid*., p. 217.
72. K. KURIBAYASHI, T. TANIGUCHI, M. YOSITAKE and S. OGAWA, *Mater. Res. Soc. Symp. Proc.* **276** (1992) 167.
73. L. CHANG, C. H. SIMPSON, D. S. GRUMMON, W. PRATT and R. LÖLÖEE, *ibid.* **187** (1990) 137.
74. L. CHANG and D. G. GRUMMON, *Scripta Metall.* **25** (1991) 2079.
75. *Idem*, *Mater. Res. Soc. Symp. Proc.* **246** (1992) 141.
76. B. WALLOS, L. CHANG and D. S. GRUMMON, *ibid.* **246** (1992) 349.
77. S. MIYAZAKI, A. ISHIDA and A. TAKEI, in "Proceedings of the International Symposium on Measurement and Control in Robotics", (IEEE, Tsukuba, 1992) p. 495.
78. A. ISHIDA, A. TAKEI and S. MIYAZAKI, *Thin Solid Films* **228** (1993) 210.
79. S. MIYAZAKI, A. ISHIDA and A. TAKEI, in "Proceedings of the International Conference on Martensitic Transformations' 92", edited by C. M. Wayman and J. Perkins, see Ref. 52, p. 893.
80. S. MIYAZAKI and A. ISHIDA, *Mater. Trans. JIM* **35** (1994) 14.
81. A. P. JARDINE, H. ZHANG and L. D. WASIELESKY, *Mater. Res. Soc. Symp. Proc.* **187** (1990) 137.
82. A. P. JARDINE and L. D. WASIELESKY, *ibid.* **187** (1990) 181.
83. J. S. MADSEN and A. P. JARDINE, *Scripta Metall. Mater.* **30** (1994) 1189.
84. C. M. SU, Z. S. HUA and M. WUTTIG, in " Proceedings of Damping of Multiphase Inorganic Materials Symposium" edited by R. B. Baghat (ASM International Pub., New York, 1993) p. 165.
85. S. Z. HUA, C. M. SU and M. WUTTIG, *Mater. Res. Soc. Symp. Proc.* **308** (1993) 33.
86. C. M. SU and M. WUTTIG, *J. Adhes. Sci. Technol.* **8** (1994) 1.
87. LI HOU and D. S. GRUMMON, *Scripta Metall. Mater.* **33** (1995) 989.
88. D. S. GRUMMON and T. J. PENCE, *Mater. Res. Soc. Symp. Proc.* **588** (1997) 331.
89. D. S. GRUMMON, LI HOU, Z. ZHAO and T. J. PENCE, *J. Phys. IV* **C8** (1995) 665.
90. R. H. WOLF and A. H. HEUER, *J. Microelectromech. Systems* **4** (1995) 206.
91. S. MIYAZAKI and K. NOMURA, in "Proceedings of the IEEE Micro Electro Mechanical Systems", (IEEE, Oiso 1994) p. 176.
92. A. ISHIDA, A. TAKEI, M. SATO and S. MIYAZAKI, *Thin Solid Films* **281-282** (1996) 337.
93. K. NOMURA and S. MIYAZAKI, "Smart Structures and Materials 1995: Smart Materials", Vol. 2441 (SPIE, Bellingham, 1995) p. 149.
94. A. ISHIDA, M. SATO, A. TAKEI and S. MIYAZAKI, *Mater. Trans. JIM* **36** (1995) 1349.
95. A. ISHIDA, M. SATO, A. TAKEI, K. NOMURA and S. MIYAZAKI, *Metall. Mater. Trans.* **27A** (1996) 3753.
96. S. MIYAZAKI, K. NOMURA and Z. HE, in "Proceedings of the 1st International Conference on Shape Memory and Superelastic Technologies", edited by A. R. Pelton, D. Hodgson and T. Duerig (SMST, Fremon, 1994) p. 19.
97. Y. NAKATA, T. TADAKI, H. SAKAMOTO, A. TANAKA and K. SHIMIZU, *J. Phys. IV* **C8** (1995) 671.
98. S. MIYAZAKI, K. NOMURA and A. ISHIDA, *ibid.* **C8** (1995) 677.
99. Y. KAWAMURA, A. GYOBU, H. HORIKAWA and T. SABURIT, *ibid.* **C8** (1995) 683.
100. K. NOMURA, S. MIYAZAKI and A. ISHIDA, *ibid.* **C8** (1995) 695.
101. LI HOU, T. J. PENCE and D. S. GRUMMON, *Mater. Res. Soc. Symp. Proc.* **360** (1995) 369.
102. T. HASHINAGA, S. MIYAZAKI, T. UEKI and H. HORIKAWA, *J. Phys. IV* **C8** (1995) 689.
103. S. MIYAZAKI, T. HOSHINAGA and K. YUMIKURA, "Smart Structures and Materials 1995: Smart Materials", Vol. 2441 (SPIE, Bellingham, 1995) p. 156.
104. S. MIYAZAKI, T. HASHINAGA and A. ISHIDA, *Thin Solid Films* **281-282** (1996) 364.
105. P. KRULEVITCH, P. B. RAMSEY, D. M. MAKOWIECKI, A. P. LEE, G. C. JOHNSON and M. A. NORTHRUP, in "Proceedings of the 1st International Conference on Shape Memory and Superelastic Technologies", edited by A. R. Pelton, D. Hodgson and T. Duerig (SMST, Fremon, 1994) p. 19.
106. L. CHANG and D. S. GRUMMON, *Philos. Mag. A*, **76** (1997) 163.
107. *Idem*, *Mater. Res. Soc. Symp. Proc.* **311** (1993) 167.
108. E. QUANDT, C. HALENE, H. HOLLECK, K. FEIT, M. KOHL, P. SCHLOßMACHER, A. SKOKAN and K. D. SKROBANEK, *Sensors and Actuators* **A53** (1996) 434.
109. A. D. JOHNSON, V. V. MARTYNOV and E. J. SHAHOIAN, "Smart Structures and Materials 1995: Smart Materials", Vol. 2441 (SPIE, Bellingham, 1995) p. 165.
110. A. D. JOHNSON, V. V. MARTYNOV and R. S. MINNERS, *J. Phys. IV* **C8** (1995) 783.
111. K. IKUTA, H. FUJISHIRO, M. HAYASHI and T. MATSUURA, in "Proceedings of the 1st International Conference on Shape Memory and Superelastic Technologies", edited by A. R. Pelton, D. Hodgson and T. Duerig (SMST, Fremon, 1994) p. 13.
112. K. N. MELTON, in "Engineering Aspects of Shape Memory Alloys", edited by T. W. Duerig, K. N. Melton, D. Stöckel and C. M. Wayman (Butterworth-Heinemann, London, 1990) p. 23.
113. W. TANG, PhD dissertation, Royal Institute of Technology (1996) p. 19.
114. S. TAKABAYASHI, K. TANINO, S. FUKUMOTO, Y. MIMATSU, S. YAMASHITA and Y. ICHIKAWA, *Jpn. J. Appl. Phys.* **35** (1996) 200.
115. A. P. JARDINE, *Mater. Res. Soc. Symp. Proc.* **360** (1995) 293.
116. J. ZHANG and D. S. GRUMMON, *Mater. Res. Soc. Symp. Proc.* **588** (1997) 451.
117. M. MERTMANN, E. HORNBOGEN and K. ESCHER, in "Shape Memory Materials'94", edited by Y. Chou and H. Tu (International Academic, Beijing, 1994) p. 556.
118. S. MIYAZAKI, to be published.
119. B. C. MUDDLE and R. M. TRAIL, in "Shape Memory Materials '94, edited by Y. Chu and H. Tu (International Academic, Beijing, 1994) p. 689.
120. K. E. SCHURCH and K. H. G. ASHBEE, *Nature* **266** (1977) 706.
121. A. ITOH, Y. MIWA and N. IGUCHI, *J. Jpn. Inst. Metals* **52** (1988) 523.
122. *Idem*, *ibid.* **54** (1990) 117.
123. Y. MIWA, A. ITOH and M. HIROK, in "Proceedings of the 28th Japan Congress on Materials Research" (SMS of Japan, Kyoto, 1985) p. 189.
124. A. ITOH, Y. MIWA and N. IGUCHI, in "Proceedings of the 31st Japan Congress on Materials Research", (SMS of Japan, Kyoto, 1988) p. 117.
125. A. H. HEUER, M. RUHLE and D. B. MARSHALL, *J. Am. Ceram. Soc.* **73** (1990) 1084.
126. M. V. SWAINT, *Nature* **322** (1986) 234.
127. B. JIANG, J. TU, T. Y. HSU, X. QI, X. ZHENG and J. ZHONG, *Mater. Res. Soc. Symp. Proc.* **246** (1992) 213.
128. P. E. REYES-MOREL, J. S. CHERNY and I. W. CHEN, *J. Am. Ceram. Soc.* **71** (1988) 343.
129. *Idem*, *ibid.* **71** (1988) 648.
130. B. C. MUDDLE and G. R. HUGO, in "Proceedings of the International Conference on Martensitic Transformations'92", edited by C. M. Wayman and J. Perkins (see Ref. 52) p. 647.
131. W. M. KRIVEN, *J. Phys. IV* **5** (1995) C8-101.
132. Y. YAMADA, *Mater. Res. Soc. Symp. Proc.* **246** (1992) 149.
133. S. TSUNEKAWA and Y. UESU, *Phys. Status Solidi A* **50** (1978) 695.
134. J. LI and C. M. WAYMAN, *Mater. Lett.* **26** (1996) 1.
135. Y. YAMADA and Y. UESU, *Solid State Commun.* **81** (1992) 777.
136. S. TSUNEKAWA, M. SUEZAWA and H. TAKEI, *Phys. Stat. Solid.* (*a*), **40** (1997) 434.

137. I. G. ZAKREVSKII, V. V. KOKORIN and A. D. SHEVCHENKO, *Fiz. Met. Metallor.* **61** (1986) 412.
138. Y. N. WANG, H. M. SHEN, M. ZHU, Y. N. HUANG, Z. F. ZHANG, Z. M. LIU and P. C. W. FUNG, *Mater. Res. Soc. Symp. Proc.* **246** (1992) 207.
139. Y. N. WANG, H. M. SHEN and M. ZHU, *Phys. Lett. A* **158** (1991) 413.
140. R. TIWARI and V. K. WADHAWAN, *Phase Trans.* **B35** (1991) 47.
141. H. M. SHEN, S. CHEN, Z. YU, Y. N. WANG, Z. X. ZHAO and P. LIU, *J. Low Temp. Phys.* **92** (1993) 181.
142. L. E. CROSS, *J. Intelligent Mater. Systems Struct.* **6** (1995) 55.
143. V. K. WADHAWAN, M. C. KERNION, T. KIMURA and R. E. NEWNHAM, *Ferroelectrics* **37** (1981) 575.
144. P. YANG and D. A. PAYNE, in "Proceedings of the International Conference on Martensitic Transformations '92", edited by C. M. Wayman and J. Perkins, (see Ref. 52) p. 719.
145. P. YANG and D. A. PAYNE, *J. Appl. Phys.* **71** (1992) 1361.
146. K. UCHINO, in "Proceedings of the MRS International Meeting on Advanced Materials", edited by K. Otsuka and K. Shimizu, Vol. 9 (MRS, Pittsburgh, 1989) p. 489.
147. K. GHANDI and N. W. HAGOOD, *AIAA J.* **33** (1995) 2165.
148. K. GHANDI and N. W. HAGOOD, "Shape Memory Ceramic Actuation of Adaptive Structures", Research Report, MIT (1995).
149. A. FURUTA, K. Y. OH and K. UCHINO, in "Proceedings of the 1990 IEEE 7th International Symposium on Applications of Ferroelectrics", (IEEE, New York, 1991) p. 528.
150. W. Y. PAN, C. Q. DAM, Q. M. ZHANG and L. E. CROSS, *J. Appl. Phys.* **66** (1989) 6014.
151. P. ROTH and E. GMELIN, *Ferroelectrics* **126** (1992) 221.
152. N. V. KASPER, A. I. AKIMOV, L. A. BLIZNYUK and I. O. TROYANCHUK, *Phys. Solid State* **37** (1995) 680.
153. I. O. TROYANCHUYK, A. I. AKIMOV, N. V. KASPER and V. V. MIKHAILOV, *ibid.* **36** (1994) 1736.
154. I. O. TROYANCHUK, H. SZYMCZAK and N. V. KASPER, *Phys. Status Solidi A* **157** (1996) 159.
155. N. V. KASPER and I. O. TROYANCHUK, *J. Phys. Chem. Solids* **57** (1996) 1601.
156. C. LIANG, C. A. ROGERS and E. MALAFEEW, "Smart Structures and Materials", AD-Vol. 24/AMD-Vol. 123 (ASME, New York, 1991) p. 97.
157. C. A. ROGERS, in "US–Japan Workshop on Smart/Intelligent Materials and Systems", edited by I. Ahmad, A. Crowson and C. A. Rogers, Technomic, Lancaster, 1990, p. 11.
158. C. LIANG, C. A. ROGERS and E. MALAFEEW, *J. Intelligent Mater. Systems Struct.* **8** (1997) 380.
159. R. F. GORDON, in "Proceedings of the 1st International Conference on Shape Memory and Superelastic Technologies", edited by A. R. Pelton, D. Hodgson and T. Duerig (SMST, Fremon, 1994) p. 115.
160. R. F. GORDON, *Mater. Technol.* **8** (1993) 254.
161. B. K. KIM, S. Y. LEE and M. XU, *Polymer* **37** (1996) 5781.
162. X. LUO, X. ZHANG, M. WANG, D. MA, M. XU and F. LI, *J. Appl. Polym. Sci.* **64** (1997) 2433.
163. H. TOBUSHI, S. HAYASHI and P. H. LIN, in "Proceedings of the International Conference on Shape Memory and Superelastic Technologies", edited by A. R. Pelton, D. Hodgson and T. Duerig (SMST, Fremon, 1994) p. 109.
164. H. TOBUSHI, H. HARA, E. YAMADA and S. HAYASHI, *Smart Mate. Struct.* **5** (1996) 483.
165. H. TOBUSHI, H. HARA, E. YAMADA and S. HAYASHI, in "Proceedings of the 3rd International Conference on Intelligent Materials", edited by P. F. Gobin and J. Tatibouet (Technomic, Lancaster, 1996) p. 418.
166. T. TAKAHASHI, N. HAYASHI and S. HAYASHI, *J. Appl. Polym. Sci.* **60** (1996) 1061.
167. Y. OSADA and B. ROSS-MURPHY, *Sci. Am.* **268** (1993) 82.
168. Y. LI and T. TANAKA, *Ann. Rev. Mater. Sci.* **22** (1992) 243.
169. M. SHIBAYAMA and T. TANAKA, *Adv. Polym. Sci.* **109** (1993) 1.
170. Y. OSADA, Y. UEOKA and J. P. GONG, in "Proceedings of the 3rd International Conference on Intelligent Materials", edited by P. F. Gobin and J. Tatibouet (Technomic, Lancaster, 1996) p. 344.
171. Z. J. ZHANG and B. Z. JANG, "Smart Structures and Materials 1995: Industrial and Commercial Applications of Smart Structures Technology", Vol. 2447 (SPIE, Bellingham, 1995) p. 26.
172. Z. HU, Y. LI, X. ZHANG and Y. CHEN, "Smart Structures and Materials 1996: Smart Materials Technologies and Biomimetics", Vol. 2716 (SPIE, Bellingham, 1996) 224.
173. H. ICHIJO, R. KISHI, E. ONE, T. SEKIYA, O. HIRASA, O. OOGANE, K. SAHARA, M. OOWADA and E. KOKUFATA, in "Proceedings of the 1st International Conference on Intelligent Materials", edited by T. Takagi, K. Takahashi, M. Aizawa and S. Miyata (Technomic, Lancaster, 1992) p. 306.
174. K. OTSUKA, in "Engineering Aspects of Shape Memory Alloys", edited by T. W. Duerig, K. N. Melton, D. Stöckel and C. M. Wayman (Butterworth-Heinemann, London, 1990) p. 36.
175. R. E. NEWNHAM, *MRS Bull.* (1997) 20.
176. A. E. CLARK, in "Ferromagnetic Materials 1", edited by E. P. Wohlfarth (North-Holland, Amsterdam, 1980) p. 531.
177. H. CHEN and H. KUBO, *Curr. Opinion Solid State Mater. Sci.* **1** (1996) 349.
178. T. KAKESHITA, K. KUROIWA, K. SHIMIZU, T. IKEDA, A. YAMAGOSHI and M. DATE, *Mater. Trans. JIM* **34** (1993) 423.
179. K. OTSUKA and K. SHIMIZU, *Int. Metals Rev.* **31** (1986) 93.
180. K. SHIMIZU and T. KAKESHITA, *ISIJ Int.* **29** (1989) 97.
181. J. R. PATEL and M. COHEN, *Acta Metall.* **1** (1953) 531.
182. M. FREMOND, "Shape Memory Alloys" (Springer, Vienna, New York, 1996) p. 3.
183. K. TANAKA, *J. Pressure Vessel Tech.* **112** (1990) 158.
184. C. LIANG and C. A. ROGERS, *J. Intelligent Mater. System Struct.* **1** (1990) 223.
185. J. G. BOYD and D. C. LAGOUDAS, *Int. J. Plasticity* **12** (1996) 805.
186. Q. P. SUN and K. C. HWANG, *J. Mech Phys. Solids* **41** (1993) 1.
187. A. L. ROYTBURD, *Mater. Res. Soc. Symp. Proc.* **246** (1992) 91.
188. A. L. ROYTBURD and J. SLUTSKER, *ibid.* **360** (1995) 299.
189. M. B. KRUGER and R. JEANLOZ, *Science* **249** (1990) 647.
190. S. M. CLARK and A. G. CHRISTY, *Phys. Rev. B* **51** (1995) 38.
191. H. SHANKARAN, S. K. SIKKA and R. CHIDAMBARAM, *High Press. Res.* **4** (1990) 393.
192. T. KAKESHITA and K. SHIMIZU, *Mater. Trans. JIM* **38** (1997) 668.
193. D. J. ERSKINE and W. J. NELLIS, *Nature* **349** (1991) 317.
194. A. M. THAKUR, N. N. THADHANI and R. B. SCHWARZ, *Metall. Mater. Trans.* **28A** (1997) 1445.
195. A. CHRISTOU, *Scripta Metall.* **4** (1970) 437.
196. M. A. MEYERS and J. R. C. GUIMARAES, *Mater. Sci. Eng.* **24** (1976) 289.
197. V. A. LOBODIUK, *Akad. Nauk Ukr. SSR Metallofiz.* **76** (1979) 3.
198. T. KAKESHITA and K. SHIMIZU, in "Proceedings of the International Conference on Martensitic Transformations'86" (JIM, Nara, 1987) p. 230.
199. V. D. SADOVSKY, L. V. SMIRNOV, Ye. FOKINA, P. A. MALINEN and I. P. SOROSKIN, *Fiz. Met. Metallov.* **24** (1967) 918.
200. E. SUN, D. Z. YANG and F. M. YANG, "Strong Magnetic Field-induced Martensitic Transformations", Research Report, Dalian University of Technology (1988).
201. T. KAKESHITA, K. SHIMIZU, M. ONO and M. DATE, *Mater. Trans. JIM* **33** (1992) 461.
202. T. KAKESHITA, K. KUROIWA, K. SHIMIZU, T. IKEDA, A. YAMAGISHI and M. DATE, *ibid.* **34** (1993) 415.

203. T. KAKESHITA, T. SABURI and K. KINDO and S. ENDO: *Jpn. J. Appl. Phys.* **36** (1997) 7083.
204. T. KAKESHITA, K. SHIMIZU, T. MAKI, I. TAMURA, S. KIJIMA and M. DATE, *Scripta Metall.* **19** (1985) 973.
205. R. D. JAMES and D. KINDERLEHRER, *Philos. Mag. B* **68** (1993) 237.
206. R. D. JAMES and M. WUTTIG, "Smart Structures and Materials 1996: Mathematics and Control in Smart Structures", Vol. 2715 (SPIE, Bellingham, 1996) p. 420.
207. R. D. JAMES and M. WUTTIG, *Philos. Mag. A*, **77** (1998) 1273.
208. K. ULLAKKO, J. K. HUANG, C. KANTNER, R. C. O'HANDLEY and V. V. KOKORIN, *Appl. Phys. Lett* **69** (1996) 1967.
209. K. ULLAKKO, J. K. HUANG, V. V. KOKORIN and R. C. O'HANDLEY, *Scripta Mater.* **36** (1997) 1133.
210. K. ULLAKKO, in "Proceedings of the 3rd International Conference on Intelligent Materials", edited by P. F. Gobin and J. Tatibouet (Technomic, Lancaster, 1996) p. 505.
211. K. ULLAKKO, P. G. YAKOVENKO and V. G. GAVRILJUK, "Smart Structures and Materials 1996: Mathematics and Control in Smart Structures", Vol. 2715 (SPIE, Bellingham, 1996) p. 42.
212. N. BRAITHWAITE and G. WEAVER, "Electronic Materials" (Materials in Action Series), (Alden Press, London, 1990) p. 175.
213. Z. G. WEI, R. SANDSTRÖM and S. MIYAZAKI, *J. Mater. Sci.* **33** (1998) 0000
214. S. A. SHABALOVSKAYA, V. I. ITIN and V. E. GYUNTER, in "Proceedings of the 1st International Conference on Shape Memory and Superelastic Technologies, edited by A. R. Pelton, D. Hodgson and T. Duerig (SMST, Fremon, 1994) p. 7.
215. V. I. ITIN, V. E. GYUNTER, S. A. SHABALOVSKAYA and R. L. C. SACHDEVA, *Mater. Charac.* **32** (1994) 179.
216. D. C. JILES, in "New Materials and Their Application 1990", edited by D. Holland (IOP Publishing, London, 1990) p. 365.
217. A. E. CLARK, in "Proceedings of the Conference on Recent Advances in Adaptive and Sensory Materials and their Applications", edited by C. A. Rogers and R. C. Rogers (Technomic, Lancaster, 1992) p. 387.
218. *Idem*, *Mater. Res. Soc. Symp. Proc.* **360** (1995) 171.

Received 10 September 1997
and accepted 22 April 1998